European Reviews of Chemical Research

Has been issued since 2014.
E-ISSN 2413-7243
2018. 5(1). Issued 2 times a year

Journal is indexed by: **CrossRef** (UK), **Electronic scientific library** (Russia), **Journal Index** (USA), **Open Academic Journals Index** (Russia), **ResearchBib** (Japan), **Scientific Indexing Services** (USA)

All manuscripts are peer reviewed by experts in the respective field. Authors of the manuscripts bear responsibility for their content, credibility and reliability.

Editorial board doesn't expect the manuscripts' authors to always agree with its opinion

Postal Address: 1367/4, Stara Vajnorska str., Bratislava – Nove Mesto, Slovakia, 831 04

Website: http://ejournal14.com/en/index.html
E-mail: evr2010@rambler.ru

Founder and Editor: Academic Publishing House Researcher s.r.o.

Release date 15.03.18.
Format 21 × 29,7/4.

Headset Georgia.

Order № 112.

European Reviews of Chemical Research

2018

Is. 1

C O N T E N T S

Articles and Statements

Published in the Slovak Republic
European Reviews of Chemical Research
Has been issued since 2014.
E-ISSN: 2413-7243
2018, 5(1): 3-10

DOI: 10.13187/ercr.2018.1.3
www.ejournal14.com

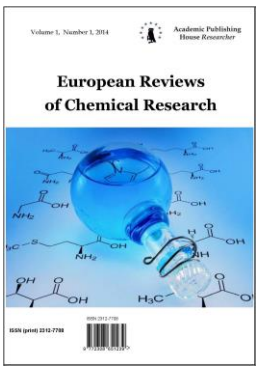

Articles and Statements

Purification of the Toxic Gaseous HCN Emissions by Oxidation in O2 Atmosphere in the Gas Phase: Quantum Chemical Modeling

Abdelilah Benallou [a, *], Habib El Alaoui El Abdallaoui [a], Hocine Garmes [b]

[a] Team of Chemoinformatics Research and Spectroscopy and Quantum Chemistry, Physical and Chemistry Lab, Faculty of Science, University Chouaib Doukkali, El Jadida, Morocco
[b] Laboratory of Bio-organic Chemistry, Department of Chemistry, Faculty of Science, University Chouaib Doukkali, El Jadida, Morocco

Abstract

HCN oxidation has been conducted in oxygen atoms, whereas the higher availability of oxygen in the atmosphere increases the HCN purification. However, this study was studied theoretically using density functional theory (DFT) method. The present work aims to evaluate the oxidation behaviour of HCN emissions in O_2 atmosphere. A detailed chemical kinetic mechanism for HCN combustion was evaluated. According to the proposed kinetic mechanism, in the ambient conditions, the oxidation of HCN proceeds mostly through the following sequence: HCN+O→NCO+H and CO_2+NH. The present modeling shows that these oxidations are preferred kinetically and energetically and are spontaneously possible in the atmosphere.

Keywords: HCN, kinetics, combustion, oxidation, theoretically.

1. Introduction

In addition to plastic waste, most solid fuels contain organic nitrogen. HCN is apparently produced from the pyrolysis of these materials. However, hydrogen cyanide (HCN) is very important in many areas of chemistry and is of major interest to experimental and theoretical chemists (Benallou, 2016; Tian et al., 2007; Benallou, 2017). Moreover, HCN vapor is released into the air from various anthropogenic sources, including the coal chemical industry (Tian et al., 2007), metal mining, synthetic fiber processing (Rahaman et al., 2007), disposal processes NO_x (Baum et al., 2007; Karlsson, 2004), rubber industries (Zhao et al., 2015). Additionally, hydrogen cyanide (HCN) plays a key role in a variety of gasoline combustion systems, and this fuel-based fossil fuel has contributed to more than 80 % of the world's energy expenditure (EEA, 2006), so hydrogen cyanide (HCN) is formed intermediately during their combustion as long as the released HCN is a function of many parameters among which must be mentioned the nature of the solid fuel; the chemical structures present in the fuel, the heating rate conditions and residence time (Glarborg et al., 2003; Potila et al., 2004; Demirbas et al., 2004). Furthermore, according to recent studies, biomass combustion provides the main source of tropospheric HCN (1.4-2.9TgN/yr), while

* Corresponding author
E-mail addresses: abdo_benallou@yahoo.fr (A. Benallou)

reactions with hydroxyl (OH) radicals and oceans uptake are responsible for its elimination (Li et al., 2000). Traces of HCN have also been measured in passenger vehicles exhausts, probably resulting from catalytic NO_x reduction reactions (Karlsson et al., 2004). In the stratosphere, HCN is oxidized by reaction with atomic oxygen and hydroxyl radicals (Kleinbohl et al., 2006).

Importantly, HCN is a very toxic gas in which 20 times more toxic than carbon monoxide (CO) and is one of the acutely toxic chemical species, HCN is extremely harmful to both health and life environment. It has been recommended by the National Institute for Occupational Safety and Health (NIOSH) that the short-term exposure limits for HCN is 4.7ppm averaged over 15 min (Chang et al., 2005). So with the cumulating emissions of HCN, it is urgent to remove the unconventional pollutant HCN in industrial waste gases.

Several treatment technologies for HCN removal have been reported (Oliver et al., 2005; Ye et al., 2009; Giménez-López et al., 2010). The sorption and catalytic oxidation are the widely used methods for the removal of HCN (Rastegar et al., 2013; Zhao et al., 2014; Shi et al., 2015). The presence of HCN gas in the atmosphere and their oxidation hypothesis by oxygen atoms in the stratosphere lead us to thinking about a possibility to purification this toxic gas by oxidation proceeds in low temperature in the gas phase, due to the lack of studies at these specific operating conditions and the increasing importance of the oxy-fuel combustion processes that represents the main source of HCN gas, while this latter can oxidize to other species not or less toxic in presence of atomic oxygen that is in excess of atmosphere. At this end, this paper will concentrate on the oxidation modeling of HCN in combustion process with the oxygen atoms in the gas phase.

2. Material and Methods

The geometry optimizations of stationary points were performed using the density functional formalism with the B3LYP exchange-correlation energy functional (Becke et al., 1993; Lee et al., 1988). All the calculations were realized with GAUSSIAN G09 program package (Frisch et al., 2009) and visualization of the output files is performed using the Gauss-View 5.0.8 software. The surface mapping was determined using a 6-311G** basis set level and the critical points (minima and transition states) were optimized and checked by calculating the intrinsic reaction coordinates (IRCs) with this basis set. All energies have been corrected for zero-point energy (ZPE) contributions calculated at the same level.

3. Results and discussion

3.1. Mechanisms studies characterization

In this paragraph, the mechanism reaction analyzing of HCN oxidation in air combustion (oxygen) to other gas not or less toxic is terminated, the HCN oxidation is carried out by one or two oxygen atoms in the gas phase, thus the relative energies of the minima and TSs are showed in Figures 3 and 4. CO, NH, CO_2, HNO, CN, NCO, OH formation were shown to be formed from HCN oxidation after a series of transformations, rearrangement, and rotation, the detailed step-by-step mechanism for the oxidation of gaseous HCN in space is depicted in Figure 1.

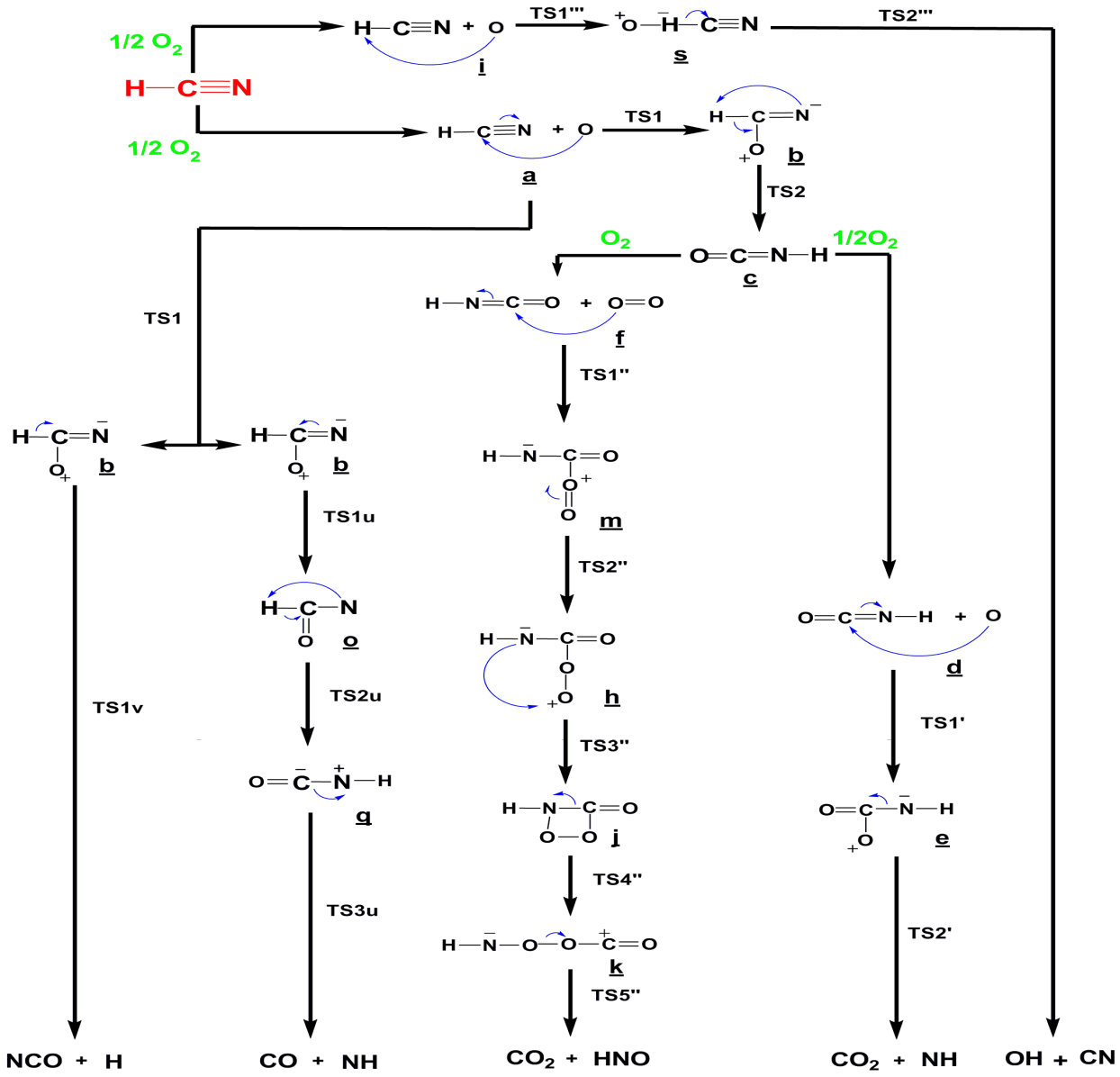

Fig. 1. Oxidation mechanisms of gaseous HCN by oxygen atoms.

Taking into account the structures mentioned in Figure 1, the minima and transition state of each complex is calculated at DFT method and 6-311G(d,p) basis set level, each TS species resulting from HCN oxidation in the gas phase are evaluated by imaginary frequency in the Hessian matrix. The distance and angle parameters of different TSs and minima are drawn and presented in figures 2 and 3.

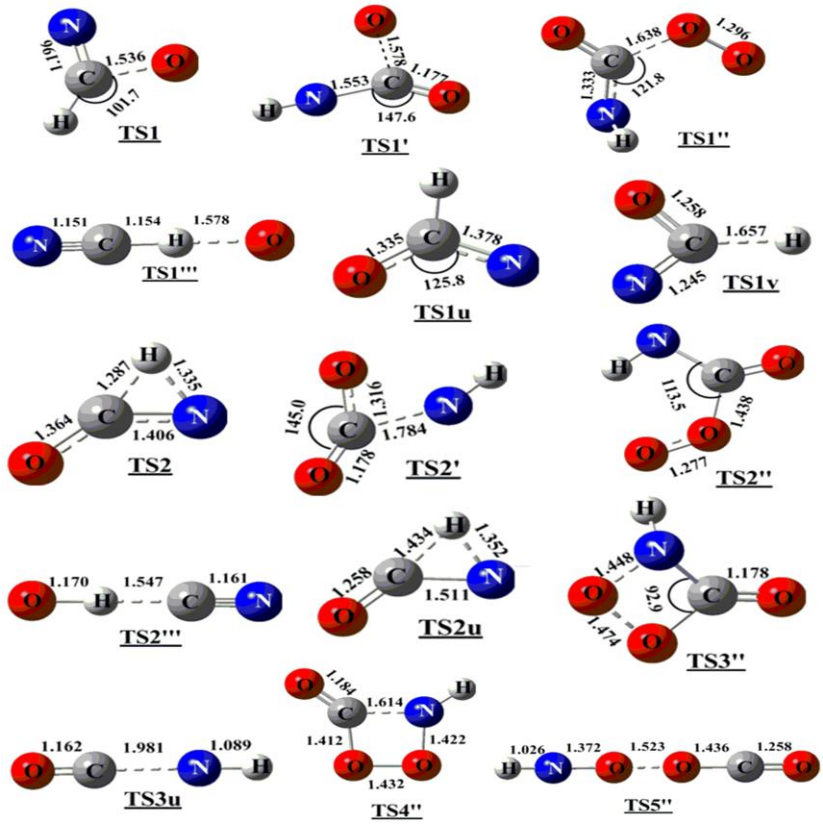

Fig. 2. Geometric structures of selected transition states of HCN oxidation optimized from DFT methods. All the transition states are planar. The distances are in Å and the angles are in degrees

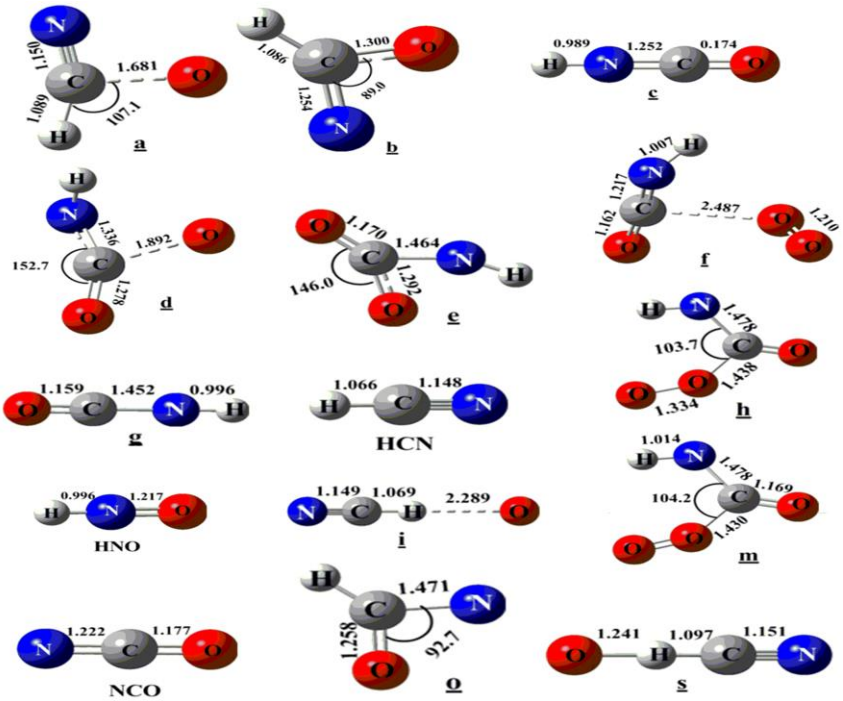

Fig. 3. Structures of the lowest-energy products of HCN oxidation optimized from DFT methods. All the minima are planar. The distances are in Å and the angles are in degrees

3.2. Barrier energy determination

The main energetic features of the oxidation of HCN is presented in this section, after mechanism pathway characterization of CO, NH, CO_2, HNO, CN, NCO, OH formation from gaseous HCN emissions in air combustion, whereas each step of oxidation process is identified energetically as well as the relative energies of different complexes (minima and transition state) shown in figures 1, 2 and 3 are determined and represented in figures 4, 5, 6, 7, 8 and 9.

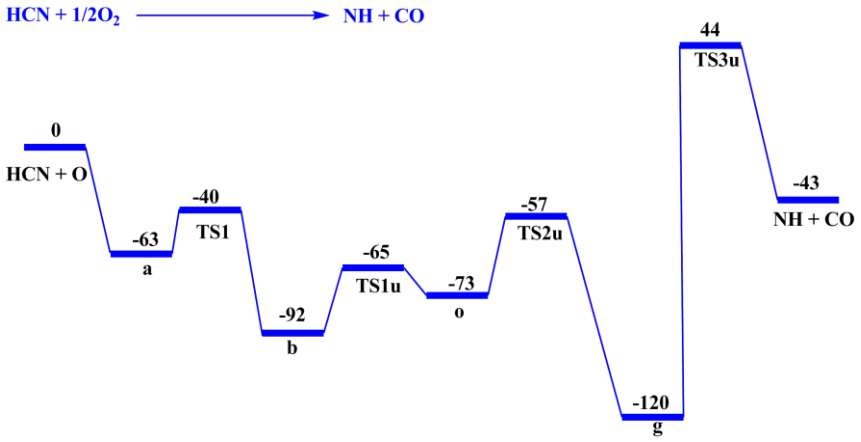

Fig. 4. DFT/6-311G(d,p) values correspond to the relative energies in kcal/mol for NH and CO formation from HCN oxidation in one atom of oxygen

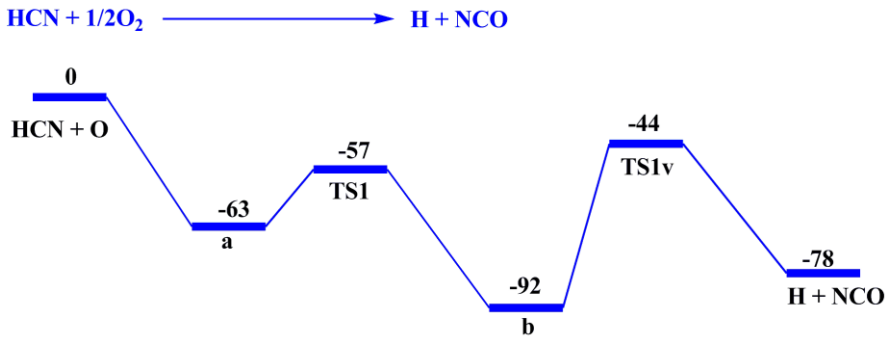

Fig. 5. DFT/6-311G(d,p) values correspond to the relative energies in kcal/mol for H and NCO formation from HCN oxidation in one atom of oxygen

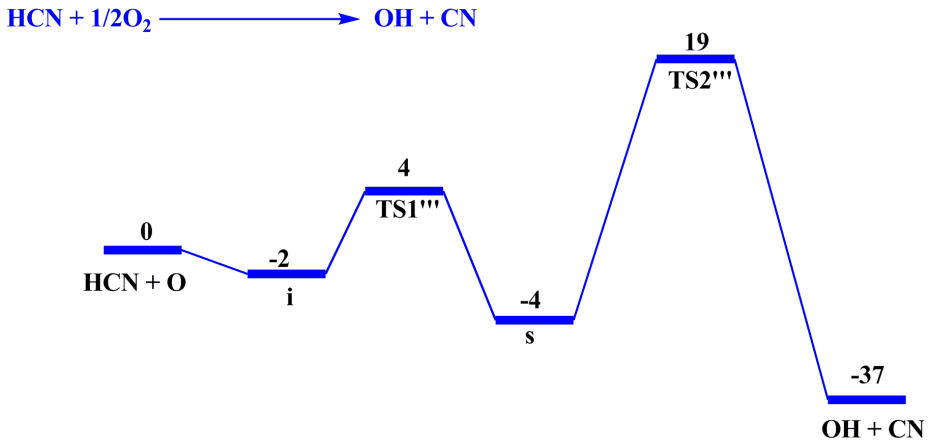

Fig. 6. DFT/6-311G(d,p) values correspond to the relative energies in kcal/mol for OH and CN formation from HCN oxidation in one atom of oxygen

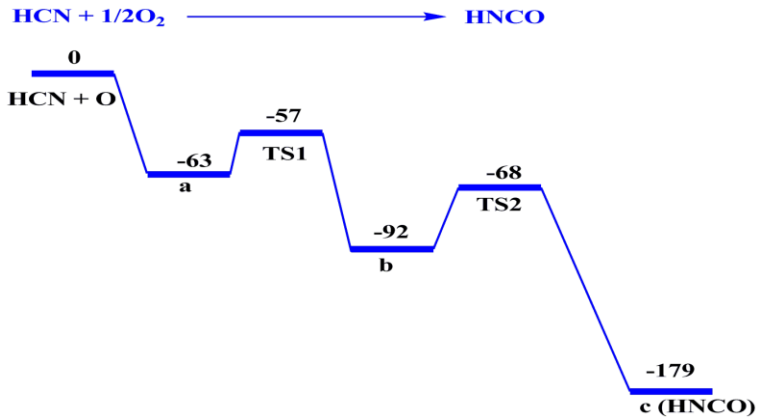

Fig. 7. DFT/6-311G(d,p) values correspond to the relative energies in kcal/mol for HNCO formation from HCN oxidation in one atom of oxygen

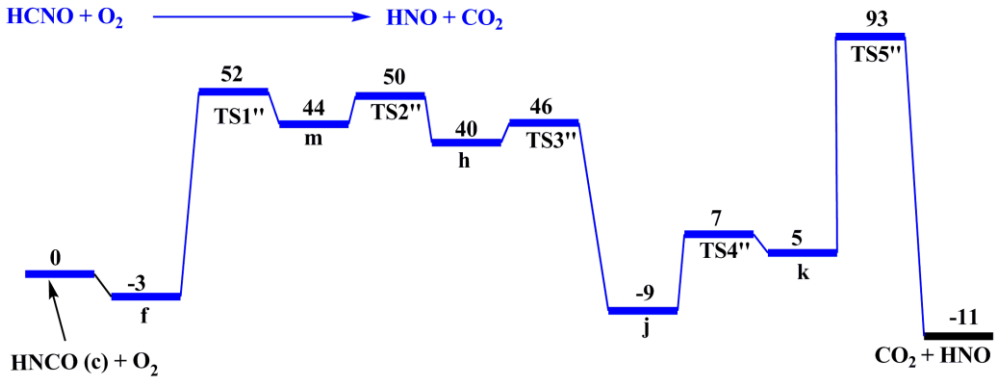

Fig. 8. DFT/6-311G(d,p) values correspond to the relative energies in kcal/mol for NHO and CO_2 formation from HCNO oxidation in two atoms of oxygen

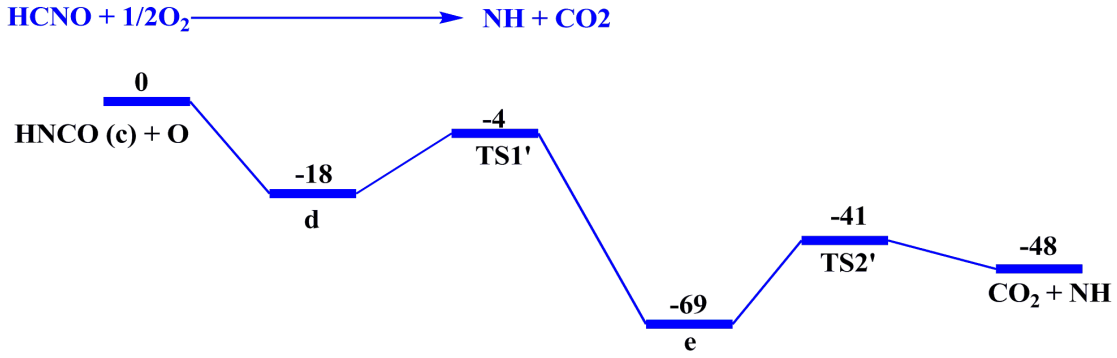

Fig. 9. DFT/6-311G(d,p) values correspond to the relative energies in kcal/mol for NHO and CO_2 formation from HCNO oxidation in one atom of oxygen

3.3. Discussion

The oxidation of HCN was studied in 1.0 atmospheric pressure and at 298K temperature, thus. Chemical kinetic reaction mechanisms of the different pathway have been proposed to represent the available data on the kinetics of HCN oxidation. However, these chemical kinetic reaction mechanisms where not certainly usable for simulating experiments over a wider range of conditions than originally tested, demonstrating the need for a more robust kinetic scheme. Although, the oxidation of HCN by O_2 or O oxygen atoms in ambient conditions and in the gas phase have been studied successfully in this paper. In this context, analyzing energetic diagrams and oxidation mechanisms lead us to conclude that HNCO, H and radical NCO are the most probable products of HCN oxidation by $½O_2$ in the gas phase because are represents the lowest

activation energies and shortest pathway processes, then they necessity less energetic contribution to started, in which need -44 and -57kcal/mol for NCO+H and HNCO formation respectively. So these oxidation reactions are endothermic and can occur spontaneously in efficiency in atmospheric space. In contrary, the other species formation OH+CN and NH+CO from gaseous HCN oxidation in one atom of oxygen, we have concluded that: on the one hand, the energetic activation is more higher in which 44 and 19kcal/mol for NH+CO and OH + CN formation respectively, and on the other hand these species are not sufficiently stables compared to the NCO+H and HNCO formation in which have values of -43kcal/mol (NH+CO), -37kcal/mol (OH+CN) versus -78kcal/mol (NCO+H) and -179kcal/mol for HNCO, therefore OH+CN and NH+CO compounds should not occur efficiently in the gas phase in atmosphere by oxidation in lonely oxygen atom but that being more likely if have a contribution for external source.

Due to stability of HNCO (-179kcal/mol) species and their high toxicity in human health, we are think to reburn this compound in lonely and twice oxygen atoms in same conditions in gas phase, so the results show that HNCO oxidation in one atom oxygen is energetically and kinetically more favourable to compare with HNCO oxidation in O_2 molecules, because this last require passing by the highest energetic activation pathway mechanism that represents the rate limiting step to be 93kcal/mol of TS5" (figure 8) for forming $HNO+CO_2$ gases. Subsequently, $HCN+1/2O_2 \rightarrow HNCO+1/2O_2 \rightarrow CO_2+NH$ and $HCN+1/2O_2 \rightarrow H+NCO$ are the most accepted mechanisms oxidation of HCN in the atmospheric gas. Since the proposed kinetic mechanisms for the oxidation of HCN were validated, a more comprehensive modeling has been needed.

Moreover, reactions burner of HCN is confirmed by calculating the enthalpy of reaction ΔHr of different compounds formation in combustion processes, this study was conducted in the same conditions of temperature and pressure, thus the results of such reaction is given below:

$HCN+1/2O_2 \rightarrow H+NCO$; ΔHr=-94.125kcal/mol
$HCN+1/2O_2 \rightarrow NH+CO$; ΔHr=-42.670kcal/mol
$HCN+1/2O_2 \rightarrow OH+CN$; ΔHr=-37.022kcal/mol
$HCN+1/2O_2 \rightarrow HNCO$; ΔHr=-181.347 kcal/mol
$HCNO+1/2O_2 \rightarrow CO_2+NH$; ΔHr=-54.593 kcal/mol
$HCNO+O_2 \rightarrow CO_2+HNO$; ΔHr=-7.530 kcal/mol

The found enthalpies energies ΔHr of oxidation reaction show that HCN oxidizes yielding H, NCO, NH, CO, OH, CN, HNCO via a complex reaction, in addition this pathway oxidation is extensively exothermic mainly of NCO and HNCO yielding to be -94.125kcal/mol and -181.347kcal/mol respectively. Thus, HCN consumption still occurs via reaction with O atoms, forming especially NCO and HNCO species in the normal conditions. However, these species can reburning in oxygen atoms to produce other products.

According to the currently accepted mechanisms, we have conclude that HCN combustion in oxygen atom is widely possible in the atmospheric conditions, can give the named gas of NCO, CO_2 and NH ($HNCO+O= CO_2+NH$) spontaneously in the gas phase.

4. Conclusion

A comprehensive detailed chemical kinetic modeling of the oxidation and combustion of HCN was performed by DFT theoretical methods. The main products formation of HCN oxidation in one or two atom oxygen's in the normal conditions are NCO, CO_2 and NH, these species are the feeble toxicity and can occur efficiently and spontaneously in the gas phase in the atmosphere of Earth. Although, the kinetic and energetic investigation show that the overall activation barrier of HCN oxidation to NCO+H and CO_2+NH is -44kcal/mol and -4kcal/mol respectively and they are more suitable for barrier activation. Therefore, the main accepted reaction paths involved in the oxidation of HCN is verified.

References

Benallou, 2016 – *Benallou A.* (2016). Understanding the most favourable dimer of HCN for the oligomerization process in the gas phase of interstellar clouds. *Comp. Theor. Chem.* 1097, 79–82.

Tian et al., 2007 – *Tian F.J., Yu J.L., McKenzie L.J., Hayashi J., Li C.Z.* (2007). Conversion of fuel-N into HCN and NH3 during the pyrolysis and gasification in steam: a comparative study of coal and biomass. *Energy. Fuel.* 21, 517–521.

Benallou, 2017 – *Benallou A.* (2017). The mechanism determination of trimer and tetramer HCN for adenine formation in the gas phase of interstellar space. *Comp. Theor. Chem.* 1101, 68–73.

Rahaman et al., 2007 – *Rahaman M.S.A., Ismail A.F., Mustafa A.* (2007). A review of heat treatment on polyacrylonitrile fiber. *Polym. Degrad. Stab.* 92, 1421–1432.

Baum et al., 2007 – *Baum M.M., Moss J.A., Pastel S.H., Poskrebyshev A.G.A.* (2007). Hydrogen cyanide exhaust emissions from in-use motor vehicles. *Environ. Sci. Technol.* 41, 857–862.

Karlsson, 2004 – *Karlsson H.L.* (2004). Ammonia, nitrous oxide and hydrogen cyanide emissions from five passenger vehicles. *Sci. Total. Environ.* 334, 125–132.

Zhao et al., 2015 – *Zhao Q., Tian S.L., Yan L.X., Zhang Q.L., Ning P.* (2015). Novel HCN sorbents based on layered double hydroxides: Sorption mechanism and performance. *J. Hazard. Mater.* 285, 250–258.

EEA, 2006 – EEA. Total energy consumption by fuel (CSI 029), assessment. Copenhagen, DK: *European Environment Agengy*, April 2006.

Glarborg et al., 2003 – *Glarborg P., Jensen A.D., Johnsson J.E.* (2003). Fuel nitrogen conversion in solid fuel fired systems. *Prog. Energy. Combust. Sci.* 29, 89–113.

Potila et al., 2004 – *Potila H., Sarjala T.* (2004). Seasonal fluctuation in microbial biomass and activity along a natural nitrogen gradient in a drained peatland. *Soil. Biol. Biochem.* 36, 1047–1055.

Demirbas et al 2004 – *Demirbas A.* (2004). Combustion characteristics of different biomass fuels. *Progr. Energy. Combust. Sci.* 30, 219–230.

Li et al., 2000 – *Li Q., Jacob D.J., Bey I., Yantosca R.M., Zhao Y., Kondo Y.* (2000). Atmospheric. Hydrogen. Cyanide. (HCN): Biomass. Burning. Source, Ocean Sink. *Geophys. Res. Lett.* 27, 357–60.

Karlsson et al., 2004 – *Karlsson H.L.* (2004). Ammonia, nitrous oxide and hydrogen cyanide emissions from five passenger vehicles. *Sci. Total. Environ.* 334–335, 125–132.

Kleinbohl et al., 2006 – *Kleinbohl A., Toon G.C., Sen B., Blavier J.F.L., Weisenstein D.K., Strekowski R.S.* (2006). Measurement of. HCN in the middle atmosphere by EOS MLS. *Geophys. Res. Lett.* 33, 11.

Chang et al., 2005 – *Chang L.P., Feng Z.H., Xie K.C.* (2005). Effect of Coal Properties on HCN and NH 3 Release During Coal Pyrolysis. *Energy. Sourc.* 27, 1399–1407.

Oliver et al., 2005 – *Oliver T.M., Jugoslav K., Aleksandar P., Nikola D.* (2005). Synthetic activated carbons for the removal of hydrogen cyanide from air. *Chem. Eng. Process.* 44, 1181–1187.

Ye et al., 2009 – *Ye P.W., Luan Z.Q., Li K., Yu L.Q., Zhang J.C.* (2009). The use of a combination of activated carbon and nickel microfibers in the removal of hydrogen cyanide from air. *Carbon.* 47, 1799–1805.

Giménez-López et al., 2010 – *Giménez-López J., Millera A., Bilbao R., Alzueta M.U.* (2010). HCN oxidation in an O2/CO2 atmosphere: An experimental and kinetic modeling study. Original research article. *Combust. Flame.* 157, 267–276.

Rastegar et al., 2013 – *Rastegar S.F., Peyghan A.A., Hadipour N.L.* (2013). Response of Si- and Al-doped graphenes toward HCN: A computational study. *Appl. Surf. Sci.* 265, 412–417.

Zhao et al., 2014 – *Zhao M., Yang F., Xue Y., Xiao D., Guo Y.* (2014). Adsorption of HCN on reduced graphene oxides: a first–principles study. *J. Mol. Model.* 20, 2214–2218.

Shi et al., 2015 – *Shi LB., Wang Y., Dong H.K.* (2015). First-principle study of structural, electronic, vibrational and magnetic properties of HCN adsorbed graphene doped with Cr, Mn and Fe. *Appl. Surf. Sci.* 329, 330–336.

Becke et al., 1993 – *Becke A.D.* (1993). Densityfunctional thermochemistry. III. The role of exact exchange. *J. Chem. Phys.* 98, 1372–1377.

Lee et al., 1988 – *Lee C., Yang W., Parr R.G.* (1988). Development of the Colle-Salvetti correlation-energy formula into a functional of the electron density. *Phys. Rev. B.* 37, 785–789.

Frisch et al., 2009 – *Frisch M.J. et al.*, GAUSSIAN 09, revision A. 02, GAUSSIAN Inc., Wallingford, CT. 2009.

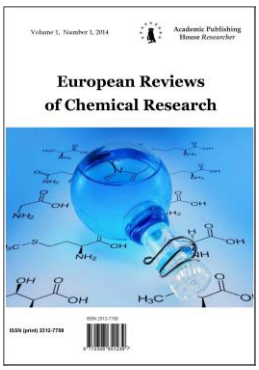

Published in the Slovak Republic
European Reviews of Chemical Research
Has been issued since 2014.
E-ISSN: 2413-7243
2018, 5(1): 11-15

DOI: 10.13187/ercr.2018.1.11
www.ejournal14.com

Extraction and Phytochemical Analysis from the Leave of Vernonia Amygdalina (Shuwaka)

I.A.A. Ibrahim [a, *], M. Chindo [b], M.M. Mohammad [a], A.A. Faisal [a], H. Musa [c]

[a] School of Science and Technology, Federal Polytechnic, Nassarawa, Nigeria
[b] Department of Science Laboratory Technology, School of Science and Technology, Abubakar Tatari Ali Polytechnic Bauchi, Nigeria
[c] Department of Microbiology, School of Science, Bauchi State University, Gadau, Bauchi, Nigeria

Abstract

The phytochemical analysis of Vernonia Amygdalina (bitter leaf) was carried out to determine the bioactive compound presenting. The plant had been use locally to treat diseases for decades. The extraction of bioactive compounds was done through aqueous and ethanol extraction. The main bioactive compounds are alkaloids, tannin. saponnin, steroids, glycoside and flavonoids. The plant also exhibited antimicrobial activity on selected microorganisms. These activities may be as a result of the metabolites present tested for and those not tested for.

Keywords: metabolites, dimethyl sulphoxide, antimicrobial, phytomedicine, parasitic.

1. Introduction

Vernonia amygadalina commonly known as bitter leaf (English) oriwo (edo) ewuro (Yoruba) and Shuwaka (Hausa) is a tropical shrub that grows up to 3 meters high in the African tropics and other parts of Africa particularly Nigeria, Cameroon and Zimbabwe (Bekele, 2015). The leaves are dark green in colour with characteristic odour and bitter tasted leafs. It is reputed to have several health benefits ; it is effective against amoebic dysentery, gastrointestinal disorders and has antimicrobial and anti-parasitic activity (Ibisi et al., 2017).

Vernonia amygadalina is a perennial herb belonging to the asterace family, the species is indigenous to tropical Africa and is found wild or cultivated all over sub-Sahara Africa (Longanga et al., 2000). The leafs are eaten after crushing and washing thoroughly , however, almost all parts of the plant are pharmacologically useful; both the root and the leaves are used in phytomedicine to treat fevers, hiccups, kidney diseases and stomach discomfort among others (Ibisi et al., 2017).

Vernonia amygadalina has various culinary and medicinal properties, the medicinal properties of the extract has bactiostastic and bacteriocidal effects on some bacteria as well as antitumorigenic properties (Akinpelu, 1999). Further studies have demonstrated hypoglycemic and hypolidimic effect of the leaves extracts in experimental animals (Nalule et al., 2013).

Many herbalist and native doctors in Africa recommend aqueous extract for their patients for treatment of a variety of ailments form emesis, nausea, diabetes, lack of appetite, dysentery ,gastrointestinal tract problems to sexual transmitted diseases and diabetes mellitus among others

* Corresponding author
E-mail addresses: iliyasuibrahim@gmail.com (I.A.A. Ibrahim)

(Nalule et al., 2013). Therefore this study was primary undertaken to confirm the acclaimed antimicrobial effects of Vernonia amygdalina in Nigeria.

2. Materials and methods

Cold extraction was employed for the extraction process and methanol was the solvent used for the extraction.

Preparation of reagents

Wagners reagent

About 3.0 g of potassium iodide was weighed and dissolved in about 40cm^3 of distilled water; to the resulting solution of potassium iodide, 2.0 g of iodide crystal was added and properly stirred to homogenize into solution.

Mayers reagents

About 1.36 g of mercury chloride was weighed and 5.00 g of potassium iodide was weighed and dissolved in 100ml of distilled water and diluted to homogenize into solution.

Sample collection and preparation

Healthy looking fresh leaves of Vernonia amygdalina (bitter leaf) free disease were collected in the morning before sun rise in a clean polythene bag at Wuntin Dada Bauchi Local Government and was transported to the Department of Science Laboratory Technology, School of Science and Technology, AbubakarTatari Ali Polytechnic Bauchi for identification and preparation of the sample. The leaves were washed thoroughly 2-3 times with running tap water and once with sterile distilled water; the leaves were then air dried under shade and then grounded into fine powder using laboratory pistle and mortar.

Extraction

About 100 g of dried powder of plant materials was added to 200 ml of sterile distilled water and methanol 70 % w/v respectively in order to obtain water and/or methanol extracts (100 mg/mc). The extraction was done at room temperature for 24 hours for the water extraction and 74 hours for the methanol extraction (Newton et al., 2002) and the fraction purified by filtering through what man No. 1 filter paper. The stock solution of the extraction was then sterilized by filtration through milli pore membrane filters of 0.45 hm pore size. The sterile extracts obtained were then stored sterile in the refrigerator at 4^{o}C until required.

Phytochemical analysis

Phytochemical analysis of the leaves extracts for the presence of some secondary metabolites was done using standard procedures.

Test for tannins

About 3 g of sample was boiled in 50ml of distilled water for 30minutes on a hot plates. The mixture was filter and a portion of the filtrate was dilute with sterile water in a 1.4 and 3 drops of 10 % ferric chloride solution was added. A blue colour indicates the presence of tannin.

Test for flavonoids

5 g of sample was weighed and dissolved completely with acetone, the residue on a water bath. The mixture was filter and the filtered was used for the test. 5 ml of 10 % of sodium hydroxide was added to an equal volume of the detained water extracts. A yellow solution indicates the presence of flavonoids.

Test for alkaloids

2 ml of sample extracts was measured in a test-tube to which picric acid solution was added. The formation of orange coloration indicates the presence of alkaloids.

Test for saponins

1 g of sample was weighed into a conical flask in which 10ml of sterile distilled water was added and boiled for 5minutes, the mixture was filtered and 5 ml to 10 ml of sterile distilled water was added in a test tube and was taped and shaken vigorously for about 30 seconds. And it was allowed to stand for half for hour. The honey comb indicates the presence and saponin.

Test for glycoside

25 ml of sulphuric acid was added to extract a test tube and boiled and then 5 ml of fehling solution A and B was added. A brick red precipitate for reducing indicate the presence of glycoside.

Antimicrobial activity

The antimicrobial activity was determined using well diffusion assay(Ekaiko et al., 2016). Dimethyl sulphoxide (DMSO) was used as a negative control and stereptomycine and ciprofloxacine (10/disc) were used as a positive control for bacteria strains and photercine B and nystatin were used as a positive control for fungi, the were done in triplicate bacteria culture were incubated at 37°C for 24 hours while the other fungi cultures were incubated at (30-32°C) for 48 hours, solution of 10mg/ml of sterptomycineciproflaxacine, nystatine and amphoteincin B were used as a standard for comparison. Antimicrobial activity was determined by measurement of zone of inhibition(Gumgumjee, Hajar, 2012).

Extraction preparation for bioassay analysis

About 1ml of the culture (previously) diluted 10^7 (fulme) was inoculated into 20 ml of molten nutrient ager in a petri plate and then spread uniformly using a sterile and a cork borer (5 mm in diameter was used to make wells on media in the plates for introduction of extract).

One hundred microliters 4 mg/ml of each extracts prepared in 20 % (DMSO) were introduced into wells. Each extracts was introduced into each hole in triplicate. The plates were kept at room temperature for extracts to diffuse in to the media before it was placed in the incubator at 37°C for 24 hours. The relative susceptibility of the organism to extract is indicated by clear zones of inhibition produced after incubation. Diameters of inhibition zones were measured by calculating the difference between cork borer (5 mm) and the diameters of the inhibition. Chloramphenicol and dimethyl sucohoxide were used positive control and negative control respectively (Adetunji et al., 2013).

Preparation of the media

The powdered agar media was mixed with water and steam to dissolve the agar and then were sterilized in a autoclave at 121°C and subsequently allowed to cool about 45 % (a temperature of which the agar remain molten in preparing the plate), some 15-20 ml of the molten agar media were poured into the sterile labeled petri dishes then stored closed upside down in a refrigerator at 4°C.

Inoculation and application of the extracts

The standard method for preparing inoculums designed by national committees for clinical laboratory standard (1990) was followed. A sterile loop was used to pick five colonies of each of the test organism into different labeled test tube containing 5ml nutrient broth.

The broth culture was inoculated over night at 37°C for the bacteria and room temperature for the fungi until a slightly visible turbidity compared to 0.5ml faland stranded (1.5x108cfo(ml).

Minimum inhibitory concentration (MIC)

The initial concentration of the plant extracts (100 g/ml) was diluted using double fold serial dilution by transferring 5 ml of the sterile plant extracts 9 stock solutions into 5 ml of nutrient broth to obtain different concentration of extracts. The process was repeated several times to obtain other dilution. 25 mg/ml, 12mg/ml have obtain different concentrations of extracts, each concentration inoculated with 0.1ml of the standardized bacterial cell suspension and inoculated at 37°C for 24 hours, the growth of the inoculums in broth is indicated by turbidity of broth and the growth of the test organisms were taken as the minimum inhibitory concentration (MIC).

3. Result and discussion

Table 1. Phytochemical analysis of Vernonia amygdalina

S/N	PHYTO CONSTITUENT	ETHANOL	WATER
1	Saponin	++	+
2	Tannin	++	+
3	Flavonoids	++	+
4	Alkaloids	+	+
6	Glycoside	+	+

Key: + = present
- = absent (not detected)

Table 2. Antimicrobial activity of *V amygdalina*

TEST ORGANISM	ETHANOL EXTRACTS zone of inhibition (mm)	AQUEOUS EXTRACTS zone of inhibition (mm)
Escherichia coli	11.3	12.5
Pseudomonas aeruginosa	10.8	12.2
Klebsiella SPP	11.4	11.8
Staphylococcus aureus	11.4	11.4
Candida	11.4	11.8

Qualitative phytochemical screening revealed the presence of natural products in the extracts, both ethanol and water leaf extracts of *Vernonia amygdalina* were found to contain all the phytochemicals tested for. These phytochemicals were all found to be present in both ethanol and water leaf extracts of *Vernonia amygdalina,* this may be attributed to similarity in their polarity indexes.

The extracts exhibited antimicrobial activity by inhibiting the growth of test organisms by their respective zones of inhibition.

The antimicrobial activity may be attributed as a result of the secondary metabolites tested for and those present that were not tested for. These metabolites have been shown to exhibit medicinal and antimicrobial properties(Senguttuvan et al., 2014; Iqbal et al., 2015; Qadir et al., 2015).

References

Adetunji, 2013 – *Adetunji, C.O., Olaniyi, O.O., Ogunkunle, A.T.J.* (2013). Journal of Microbiology and Antimicrobials Bacterial activity of crude extracts of Vernonia amygdalina on clinical isolates. *Journal of Microbiology and Antimicrobials*, *5*(6), 60–64. https://doi.org/10.5897/JMA11.033

Akinpelu, 1999 – *Akinpelu, D.A.* (1999). Antimicrobial activity of Vernonia amygdalina leaves. *Fitoterapia*, *70*(4), 432–434. https://doi.org/10.1016/S0367-326X(99)00061-1

Bekele, 2015 – *Bekele, T.* (2015). Invivo Anti-Malarial Evaluation of Leaf Extract of Vernonia amygdalina Del . (Asteraceae) against Plasmodium berghei A Thesis submitted to Addis Ababa University , School of Graduate Studies , and Department of Biochemistry in Partial fulfillment of the.

Ekaiko, 2016 – *Ekaiko, M., Ajuga, M., Okeke, I. M., G, A. A., C, N. J.* (2016). Antimicrobial Effect of Chromolaena Odorata (L.) and Vernonia Amygdalina Del Leaf Extract on Clinical Isolates from Infected Wound. *IOSR Journal of Pharmacy and Biological Sciences Ver. III*, *11*(3), 2319–7676. https://doi.org/10.9790/3008-1103038386

Gumgumjee, 2012 – *Gumgumjee, N. M., Hajar, A. S.* (2012). Antimicrobial efficacy of Casuarina equisetifolia extracts against some pathogenic microorganisms. *Journal of Medicinal Plants Research*, *6*(47), 5819–5825. https://doi.org/10.5897/JMPR12.741

Ibisi, 2017 – *Ibisi, N. E., Okoroafor, D. O., Amuta, C. C.* (2017). Comparative Study of Mild Steel Corrosion Inhibition of Piper Guineense Leaves Extract and Vernonia Amygdalina Leaves Extract in Concentrated Corrosive Medium. *IOSR Journal of Applied Chemistry*, *10*(5), 70–78. https://doi.org/10.9790/5736-1005027078

Iqbal, 2015 – *Iqbal, E., Salim, K. A., Lim, L. B. L.* (2015). Phytochemical screening, total phenolics and antioxidant activities of bark and leaf extracts of Goniothalamus velutinus (Airy Shaw) from Brunei Darussalam. *Journal of King Saud University – Science*, *27*(3), 224–232. https://doi.org/10.1016/j.jksus.2015.02.003

Longanga, 2000 – *Longanga, O., Vercruysse, A., Foriers, A.* (2000). Contribution to the ethnobotanical,phytochemical and pharmacological studies of traditionally used medicinal plant in the treatment of dysentery and diarrhea in Lomela area, Democratic Republic of Congo (DRC). *J Ethnopharmacol*, *71*(3), 411–423.

Nalule et al., 2013 – *Nalule, A.S., Mbaria, J.M., Kimenju, J.W.* (2013). In vitro anthelmintic potential of Vernonia amygdalina and Secamone africana on gastrointestinal nematodes.

Agriculture and Biology Journal of North America, *4*(1), 54–66. https://doi.org/10.5251/abjna.2013.4.1.54.66

Qadir et al., 2015 – *Qadir, U., Paul, V.I., Ganesh, P.* (2015). Preliminary phytochemical screening and in vitro antibacterial activity of Anamirta cocculus (Linn.) seeds. *Journal of King Saud University - Science*, *27*(2), 97–104. https://doi.org/10.1016/j.jksus.2014.04.004

Senguttuvan et al., 2014 – *Senguttuvan, J., Paulsamy, S., Karthika, K.* (2014). Phytochemical analysis and evaluation of leaf and root parts of the medicinal herb, Hypochaeris radicata L. for in vitro antioxidant activities. *Asian Pacific Journal of Tropical Biomedicine*, *4* (Suppl 1), S359–S367. https://doi.org/10.12980/APJTB.4.2014C1030

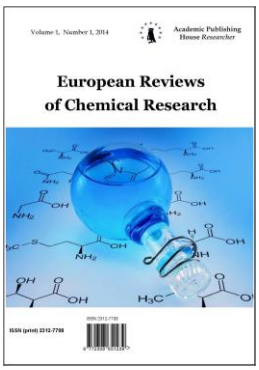

Published in the Slovak Republic
European Reviews of Chemical Research
Has been issued since 2014.
E-ISSN: 2413-7243
2018, 5(1): 16-21

DOI: 10.13187/ercr.2018.1.16
www.ejournal14.com

Phytochemical and Antimicrobial Activity of Stem Bark Extract of Ficus Plat Platyphylla Extraction and Phytochemical Analysis from the Leave of Vernonia Amygdalina (Shuwaka)

I.A.A. Ibrahim [a, *], M. Chindo [b], M.M. Mohammad [a], A.A. Faisal [a], H. Musa [c]

[a] Department of Science Laboratory Technology, School of Science and Technology, Federal Polytechnic, Nassarawa, Nigeria
[b] Department of Science Laboratory Technology, School of Science and Technology, AbubakarTatari Ali Polytechnic Bauchi, Nigeria
[c] Department of Microbiology, School of Science, Bauchi State University, Gadau, Bauchi, Nigeria

Abstract

Stem bark sample (100g and 60g) of Ficus platyphylla were thoroughly extracted with ethanol and water respectively. The qualitative phytochemical analysis of the ethanol crude extract showed the presence of saponin, tannis, flavonoids ring, cardiac glycosides and carbohydrates, steroids ring, and Alkaloids. The qualitative was justified by their colour changes with their various reagents. The extract exhibited antimicrobial activity on E coli and S aureus. This appears to because of the secondary metabolites tested for and those present but not tested for.

Keywords: inflammatory, ficus platyphylla, analgrstic, therapeutic, precursor, orthodox.

1. Introduction

Background of the study

Ficus platyphylla is a deciduous plant locally known as “Gamji” in Hausa and widely distributed through the Savannah region of West Africa coast. The plant is used by herbalist for treating several diseases such as insomnia, psychosis, depression, and as analgesic (Menezes et al., 2011).

Ficus Plattyphylla which consists of about 60 species of typical fruiting trees in the flowing plant of family moraceae. It is a large savannah tree which grows up to 60ft high with trusty or pinkish-brown bark and large grey scaly distributed in sub-Sahara Africa. The bark of the plant has been used in the treatment of asthma disease; it’s also help in flushing out contaminated blood from the body of newly delivered women, insomnia epilepsy, pain and inflammation for many years and also malaria (Beyene et al., 2016).

Medicinal plant contains substances used for the therapeutic purpose or used as a precursor for the synthesis of some drug as well as vital chemicals. The origin of the therapeutic used a herbal medicine can be trace to China about 500 years ago(Narendhiran et al., 2014), a large part of the world population still relies on plant as they affordable sources of medicine Herbalists and indigenous healer have used botanical medicines traditionally worldwide for the prevention and treatment of different pathogens, traditionally medicine is of immense value in the healthcare

* Corresponding author
E-mail addresses: iliyasuibrahim@gmail.com (I.A.A. Ibrahim)

system of developing countries, and the world health organization (Narendhiran et al., 2014) estimated that more than 80 % of health care need in this countries are met through traditional healthcare practice (World Health Organisation, 2001).

This is may be possibly because it affordability and accessibility is more than that of orthodox medicine (Beyene et al., 2016).

A lot of herbs have been used traditionally to treat infertility, malara, cholera, tuberculosis, myelin (meca), Discorea villosa (wild yam) Ficus platyphylla has been used for this purpose.

Ficus platyphylla has been evaluate for the scientific basic for the use of this plant in traditional medicine for the treatment of Central Nervous System (C.N.S) disorders(Qadir et al., 2015). The extract of ficus platyphylla has been reported to possess Analgesis(Iqbal et al., 2015), an inflammatory and anti contraceptive activities (Wakeel et al., 2004). Further investigation reported the use of the stem bark in the treatment of tuberculosis, the extract plant are used in Huasa ethnol medicine of Northern Nigeria for the treatment of various ailments (Odey et al., 2012).

2. Main part

Experimental

Preparation of reagents

Warner's reagent

About 3.0 g of potassium iodide was weighed and dissolved in about 40cm^3 of distilled water. To the resulting solution of potassium iodide, 2.0 g of iodide crystal was added and properly stirred to homogenize into solution. This was transferred into 100cm^{3}volumetric flask and filled up to the mark with distilled water.

Mayer's reagent

The Mayer's reagent is freshly prepared by dissolving a mixture of mercuric chloride (1.36 g) and of potassium iodide (5.00 g) in water (100.0 m).

Sample collection and preparation

The sample collection

The stem bark of the plan ficus platyphylla was collected at MARA Ward, Rimin Zayam, Toro Local Government Area, Bauchi State, Nigeria.

Preparation of sample

The plant sample was air dried under shade for about two weeks then tightly parked inside a clean and sterilized paper bag and kept in the laboratory until it required.

Extraction

Ethanol extraction

The 100ml of ethanol was added to 50 g of the Powder and homogenized in a conical flask. The mixture was stirred and allowed to stand for 48 hours at room temperature by occasionally mixing. After 48 hours the mixture was filtered using a watchman NO: 4filter paper, the filtrate was allowed to evaporate to dryness in a water bath at 60^{o}c and the residue was air dried. The percentage yield was calculated accordingly.

Aqueous extraction

A 60g of the powdered plant sample was soaked in 500cm^3 of distilled water; the mixture was heated to boil for 40minutes and then allowed to stand for 48 hours at room temperature. The mixture was filtered thoroughly with a watchman NO4 filter paper and the filtrate heated in a water bath until it completely dried. The residue was weighted and the percentage yield was calculated.

Preparation of reagents

Wagners reagent

About 3.0g of potassium iodide was weighed and dissolved in about 40cm^3 of distilled water; to the resulting solution of potassium iodide, 2.0g of iodide crystal was added and properly stirred to homogenize into solution.

Mayers reagents

About 1.36 g of mercury chloride was weighed and 5.00g of potassium iodide was weighed and dissolved in 100ml of distilled water and diluted to homogenize into solution.

Sample collection and preparation

Healthy looking fresh leaves of Vernonia amygdalina (bitter leaf) free disease were collected in the morning before sun rise in a clean polythene bag at Wuntin Dada Bauchi Local Government and was transported to the Department of Science Laboratory Technology, School of Science and

Technology, AbubakarTatari Ali Polytechnic Bauchi for identification and preparation of the sample. The leaves were washed thoroughly 2-3 times with running tap water and once with sterile distilled water; the leaves were then air dried under shade and then grounded into fine powder using laboratory pistle and mortar.

Extraction

About 100 g of dried powder of plant materials was added to 200ml of sterile distilled water and methanol 70 % w/v respectively in order to obtain water and/or methanol extracts (100 mg/mc). The extraction was done at room temperature for 24 hours for the water extraction and 74 hours for the methanol extraction (Newton et al., 2002) and the fraction purified by filtering through what man No. 1 filter paper. The stock solution of the extraction was then sterilized by filtration through milli pore membrane filters of 0.45 hm pore size. The sterile extracts obtained were then stored sterile in the refrigerator at 4^{o}C until required.

Phytochemical analysis

Phytochemical analysis of the leaves extracts for the presence of some secondary metabolites was done using standard procedures.

Test for tannins

About 3g of sample was boil in 50 ml of distilled water for 30minutes on a hot plates. The mixture was filter and a portion of the filtrate was dilute with sterile water in a 1.4 and 3 drops of 10 % ferric chloride solution was added. A blue colour indicates the presence of tannin.

Test for flavonoids

5 g of sample was weighed and dissolved completely with acetone, the residue on a water bath. The mixture was filter and the filtered was used for the test. 5 ml of 10 % of sodium hydroxide was added to an equal volume of the detained water extracts. A yellow solution indicates the presence of flavonoids.

Test for alkaloids

2 ml of sample extracts was measured in a test-tube to which picric acid solution was added. The formation of orange coloration indicates the presence of alkaloids.

Test for saponins

1 g of sample was weighed into a conical flask in which 10ml of sterile distilled water was added and boiled for 5 minutes, the mixture was filtered and 5 ml to 10ml of sterile distilled water was added in a test tube and was taped and shaken vigorously for about 30 seconds. And it was allowed to stand for half for hour. The honey comb indicates the presence and saponin.

Test for steroid

The crude extract each was mixed with 2ml of chloroform and concentrated hydrochloric acid was added side wise. The appearance of red colour produced in the lower chloroform layer indicated the presence of steroid.

Test for Anthraquanones

0.5 mg of each extract was put into a dry test tu be and 5ml of chloroform was added while shaking for about 5minutes. The mixture was then filtered and the filtrate was shaken with an equal volume of 100 % ammonia solution. The appearance of a pink, violet colour in ammonia layer indicated the presence of free anthraquanones.

Test for carbohydrate

5 mg of each extract were heated with concentrated sulfuric acid. The appearance of blackening effervescence indicated the presence of carbohydrate.

Test for Cardiac glycoside

Crude extract was mixed with 2ml of chloroform and 2ml of acetic acid. The mixture was cooled in ice sulfuric acid was carefully added. A change of colour from violet to blue to greenish indicated the presence of glycosides.

Preparation of the media

The powdered agar media was mixed with water and steam to dissolve the agar and then were sterilized in a autoclave at 121^{o}C and subsequently allowed to cool about 45 % (a temperature of which the agar remain molten in preparing the plate), some 15-20ml of the molten agar media were poured into the sterile labeled petri dishes then stored closed upside down in a refrigerator at 4^{o}C.

Inoculation and application of the extracts

The standard method for preparing inoculums designed by national committees for clinical laboratory standard (1990) was followed. A sterile wire loop was used to pick five colonies of each of the test organism into different labeled test tube containing 5ml nutrient broth.

The broth culture was inoculated over night at 37°C for the bacteria and room temperature for the fungi until a slightly visible turbidity compared to 0.5ml faland stranded (1.5x108cfo(ml).

Minimum inhibitory concentration (MIC)

The initial concentration of the plant extracts (100 g/ml) was diluted using double fold serial dilution by transferring 5 ml of the sterile plant extracts 9 stock solutions into 5ml of nutrient broth to obtain different concentration of extracts. The process was repeated several times to obtain other dilution. 25 mg/ml, 12 mg/ml have obtain different concentrations of extracts, each concentration inoculated with 0.1ml of the standardized bacterial cell suspension and inoculated at 37°C for 24 hours, the growth of the inoculums in broth is indicated by turbidity of broth and the growth of the test organisms were taken as the minimum inhibitory concentration (MIC).

Extraction preparation for antimicrobial activity

16ml nutrient ager plates that has been checked for sterility were seeded with 0.1 of an overnight broth culture of each bacterial isolate in sterile plates The stem bark plates were allowed to set after a uniform distribution of the bacterial isolate following slow rotation of the plates. A standard sterile cork borer of 6ml diameter was used to cut uniform wells on the surface of the ager. The wells filled with 0.1ml of each extracts and allowed to stand for 1hour at room temperature to allow proper diffusion of the extract to occur under sterile conditions. All the plates were incubated at 37°c for 24hours and observed for the zone of inhibition. A zone inhibition and the diameter are measured in millimeters.

Inoculation and application of the extract

The stem bark extract of the plant at different concentration were arranged radically and extract of the plant at different concentration were arranged radically and pressed firmly on to the inoculated ager surface to ensure even contact. Each disc was sufficiently space out and kept at least 15 mm from the edge of the plate to prevent overlapping of zones. The plate inoculated aerobically 37°C for 18 hours. Diameter of zone inhibition was measure using millimeter rule.

Determination of minimum inhibitory concentration (MIC)

Grade concentration of the ethanolic extracts 5ml each were mixed with melted (45°C) 5 ml of double strength Mueller-Hilron ager and poured aseptically into sterile plate. The plates were allowed to set sterile paper discs in duplicates were aseptically placed equidistantly on the set ager. Thereafter 10NL of the standardized bacterial cultures were inoculated on the sterile paper disc aseptically. The plates were allowed to stand for 1 hour and then incubated at 37₀C for 18 hours. Ciprofloxacin was used as standard antibiotics. This procedure was carried out for fungal culture.

3. Results

Table 1. Phytochemical analysis of Ficus playtyphylla

Metabolic	Water extract	Ethanol extract
Saponin	+	+
Tannin	+	+
Flavonoid	-	+
Anthraquanone	-	-
Carbohydrate	+	+
Alkaloid	+	-
Steroid Ring	+	+
Cardiac Glycoside	-	+

Key:

+ = Present

- = Absent

Table 2. Mass of Reactants and Residue

SOLVENT	MASS OF SAMPLE	MASS OF RESIDUE	MASS OF EXTRACT
Water	60g	49.9g	10.1g
Ethanol	100g	83.4g	16.6g

Table 3. Physical Properties of Solvent

SOLVENT	B.P	M.P	COLOUR & TEXTURE	DENSITY
Water	100°C	O°C	Maroon & Solid	100kg/m^3
Ethanol	78.37°C	-114°C	Reddish brown & solid	0.789g/cm^3 at 25°C

Table 4. Antimicrobial Effect of Extract

TEST ORGANISM	CONCENTRATION (mg/ml)	ZONE OF INHIBITION	
	10^{-1}	Water extract	Methanol extract
	10^{-2}	21.00MM	23.00mm
S. Aureus	10^{-3}	17.00MM	18.00mm
	10^{-4}	X	X
	10^{-5}	X	X
	10^{-1}	22.00mm	24.00mm
	10^{-2}	18.00mm	19.00mm
E. Coli	10^{-3}	X	X
	10^{-4}	X	X
	10^{-5}	X	X

Discussion

The qualitative test have been carried out using, ficus platyphylla stem bark extracts and it revealed various composition of phytochemicals, crude extract, and antimicrobial Assay of ficus platyphylla demonstrated the presence of most of the phytochemicals tested. Both the ethanol and water extract revealed the presence of saponins, tannins, flavonoids, alkaloids, cardiac glycoside, steroids, and carbohydrates. This may be so because of the relative similarity in polaritiy (Odey et al., 2012). While antheraquinones is absent in both aqueous and ethanol extract of the plant.

The bioassay of the methanol and water extracts of Ficus platyphylla (Stem bark) gave a minimum inhibitory concentration at 21.00 mm and 22.00 mm for Staphylococcus aureus and Escherichia, coli respectively. The result agrees with other research in similar area in the antimicrobial effects of secondary metabolites(Beyene et al., 2016).

References

Beyene, 2016 – *Beyene, B., Beyene, B., Deribe, H., Science, C.* (2016). Review on Application and Management of Medicinal Plants for the Livelihood of the Local Community, *22*, 33–39.

Iqbal, 2015 – *Iqbal, E., Salim, K. A., Lim, L.B.L.* (2015). Phytochemical screening, total phenolics and antioxidant activities of bark and leaf extracts of Goniothalamus velutinus (Airy Shaw) from Brunei Darussalam. *Journal of King Saud University – Science*, *27*(3), 224–232. https://doi.org/10.1016/j.jksus.2015.02.003

Menezes et al., 2011 – *Menezes, C., Kunal, G., Reema, N., Satyanarayana, D., Jagadish, K.* (2011). Analgesic and Anti-inflammatory Activity of Ficus glomerata in Experimental Animal Models, *4*(3), 11–14.

Narendhiran et al., 2014 – *Narendhiran, S., Mohanasundaram, S., Arun, J., Rannjith, R.V, Saravanan, L., Catherine, L., Subathra, M.* (2014). Phytochemical Screening and Antimicrobial Activity of. *Journalrepository.Org*, *6*(1), 1–4. Retrieved from http://www.journalrepository.org/media/journals/BBJ_11/2016/Sep/ Akacha1622016BBJ28905.pdf

Odey et al., 2012 – *Odey, M.O., Iwara, I.A., Udiba, U.U., Johnson, J.T., Asenye, M.E., Victor, O.* (2012). Preparation of Plant Extracts from Indigenous Medicinal Plants. *International Journal of Science and Technology*, *1*(12), 688–692.

Qadir et al., 2015 – *Qadir, U., Paul, V.I., Ganesh, P.* (2015). Preliminary phytochemical screening and in vitro antibacterial activity of Anamirta cocculus (Linn.) seeds. *Journal of King Saud University – Science*, *27*(2), 97–104. https://doi.org/10.1016/j.jksus.2014.04.004

Wakeel et al., 2004 – *Wakeel, O.K., Aziba, P.I., Ashorobi, R.B., Aderibigbe, A., Awe, E.O.* (2004). Neuropharmacological Activities of Ficus Platyphylla Stem Bark in Mice, *7*, 75–78.

World Health Organisation, 2001 – World Health Organisation (2001). Legal Status of Traditional Medicine and Complementary/Alternative Medicine: A Worldwide Review. *Essential Medicines and Health Products Information Portal: A World Health Organization Resource*, 200. https://doi.org/j

Published in the Slovak Republic
European Reviews of Chemical Research
Has been issued since 2014.
E-ISSN: 2413-7243
2018, 5(1): 22-29

DOI: 10.13187/ercr.2018.1.22
www.ejournal14.com

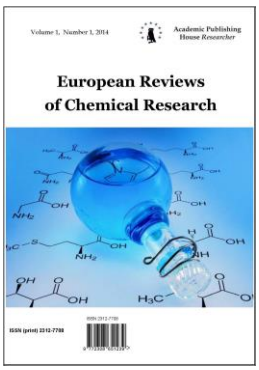

A Regioselective and Stereoselective Synthesis of 2,5-Dichloro-2,5,9,9-tetramethyl-decahydro-benzocycloheptene via Stepwise addition Reactions between α-himachalene and HCl: Experimental and Theoretical Study

N. Ourhriss [b, c], A. Zeroual [a, b, *], C. A. Gadhi [d], A. Benharref [b], A. Abourriche [c], A. Bennamara [c], A.El Hajbi [a]

[a] Laboratory of Physical Chemistry, Faculty of Science, Chouaïb Doukkali University, El Jadida, Morocco
[b] Laboratory of Biomolecular Chemistry, Natural Substances and Reactivity, URAC 16, Faculty of Sciences Semlalia, Cadi Ayyad University, Marrakech, Morocco
[c] Biomolecular and Organic Synthesis Laboratory, Faculty of Sciences Ben M'sik Casablanca, Hassan II University, Morocco
[d] Laboratory of Biotechnology, Valorization and Protection of Vegetable Resources (Biote V.R.V), Faculty of Sciences Semlalia, Cadi Ayyad University, Marrakech, Morocco

Abstract

2,5-Dichloro-2,5,9,9-tetramethyl-decahydro-benzocycloheptene has been prepared using addition reaction of α-himachalene and HCl. In addition, this reaction have been theoretically studied using DFT methods at the B3LYP/6–31G(d) level of theory. The comparatively low activation energies and Parr functions of the nucleophilic α-himachalene and 3,7-dichlorohimachalane, as well as electrophilic Parr functions of the electrophilic HCl, expounding the regio- and stereospecific experimentally observed.

Keywords: Addition reaction, α-himachalene, DFT, Regioselective, Stereoselective.

1. Introduction

Essential oils have many biological activities. In herbal medicine, they are used for their antiseptic properties against infectious diseases of bacterial origin, for example against endocanalar bacteria or at the level of the vaginal microflora (Arnal-Schnebelen et al., 2004) and of fungal origin against dermatophytes (Kurkin, 2003). However, they also have cytotoxic properties (Sivropoulou et al., 1996) which bring them closer to antiseptics and disinfectants as broad spectrum antimicrobial agents. In the phytosanitary and agro-food fields, essential oils or their active compounds could also be used as protection agents against phytopathogenic fungi (Zambonelli et al., 2004) and microorganisms invading foodstuffs (Mangena et al., 1999).

To improve the chemical and biological properties, we have studied the action of gaseous hydrochloric acid on the sesquiterpene α-himachalene isomer gives regioselectively and stereoselectively a dichloride named 3,7-dichlorohimachalane P-2a in the crystallized solid form (Figure 1).

* Corresponding author
E-mail addresses: zeroual19@yahoo.fr (A. Zeroual)

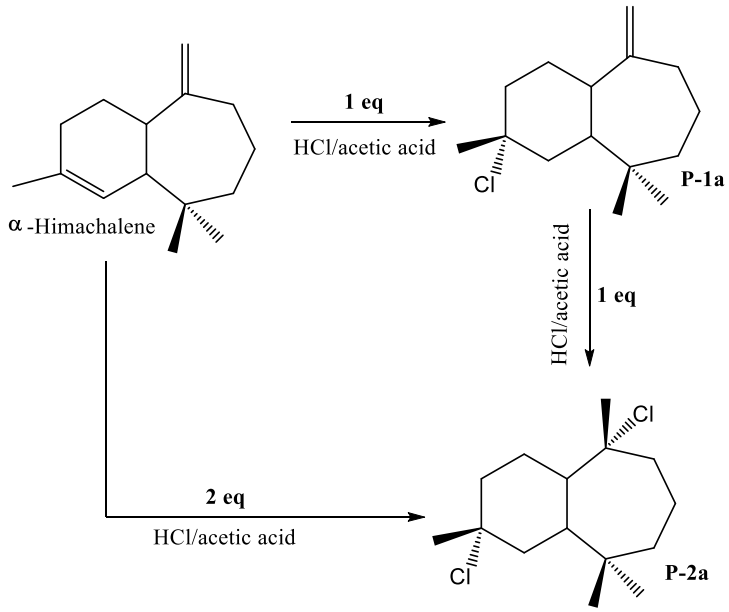

Fig. 1. Continuation synthesis procedure of 3,7-dichlorohimachalane

Experimental techniques and theoretical methods have been complementing each other yielding an accelerated progress in the understanding of materials at atomistic dimensions. We will concentrate in this work; our aim is to explicate the mechanism, regioselectivity and stereoselectivity experimentally obtained.

2. Experimental

General procedure for the preparation of products

α-himachalène, (1 g, 4.9 mmol), dissolved in 10 ml of acetic acid, was treated with a stream of hydrochloric acid gas until a solid product appeared. The mixture was allowed to stand at 273 K for 12 h and then at room temperature for 2 h. After filtering under reduced pressure, the compound (3,7-dichlorohimachalane) was obtained in a yield of 85%. After evaporation of hexane, the appropriate crystals are obtained.

(1S,3R,6S,7R)-3,7-Dichloro-trans-himachalane

(C15H26Cl2)Pf= 118-120 °C (Solide blanc) (hexane), 80%RMN 1H (300 MHz, CDCl3) δ (ppm): 0.87, 1.04 (H14, H15, s, s); 1.58, 1.6 (H12, H13 , s,s) RMN 13C(75 MHz, CDCl3) δ (ppm): 20.60 33.19 (C14, C15) ; 34.44, 35.76 (C12, C13) ; 71.15 (C3) ; 75.98 (C7) ; 46.26 (C6) ; 51.55 (C1) ; 36.34(C11).

3. Computational methods

The geometric parameters for the reactants, TSs, and products of the reactions studied were fully optimized using the density functional theory (DFT) method (Nacereddine et al, 2015). The calculations were performed at B3LYP (Becke, 1993) level with the 6-31G (d) basis set (Rassolov et al., 2009). All calculations reported in this paper were performed on the Gaussian 09 (Frisch et al., 2009), using Berny's algorithm (Schlegel, 1982). Atomic electronic populations and reactivity indices were calculated using natural population (NPA). The global electrophilicity index (Parr et al., 1999) ω, was given by the following expression $\omega = \frac{\mu^2}{2\eta}$, in terms of the electronic chemical potential μ and the chemical hardness η. Both quantities could be approached in terms of the one-electron energies of the frontier molecular orbital HOMO and LUMO, ε_H and ε_L as $\mu = \frac{\varepsilon_H + \varepsilon_L}{2}$ and $\eta = \varepsilon_H - \varepsilon_L$, respectively. The empirical nucleophilicity index N (Domingo et al., 2009) based on the HOMO energies obtained within the Kohn-Sham (Kohn *et al.*, 1965), and defined as $N = E_{HOMO}(Nu) - E_{HOMO}(TCE)$. the nucleophilicity was referred to tetracyanoethylene (TCE). Electrophylic P_k^+ and nucleophilic P_k^- Par functions were obtained through analysis of the Mulliken atomic spin density (ASD) of the radical anion and radical cation of the reagents. (El Haib

et al., 2018; Zeroual et al., 2017; Zoubir et al., 2017; El Idrissi et al., 2017; Ourhriss et al., 2017; El Idrissi et al., 2017; Zeroual et al., 2015; Barhoumi et al., 2015; Ryachi et al., 2015).

Geometry optimization calculations were carried out to obtain the global minima for the reactants and products, and to locate the saddle point for the TS. Stationary points were characterized by frequency calculations. All reactants and products had positive Hessian matrices. All TSs had only one negative eigen value in their diagonalized Hessian matrices, and their associated eigenvectors were confirmed to correspond to motion along the reaction coordinate under consideration. TSs were located using the (QST2) algorithm. Intrinsic reaction coordinate (IRC) calculations were carried out for all events to verify that the localized TSs connected with the corresponding minimum stationary points associated with reactants and products (Fukui, 1970).

4. Discussion

This section was divided into three parts: (1) an analysis of the reactivity indices of the reagents. (2) Next, an analysis of the reactivity local indices of the reagents. (3) Finally kinetic study.

4.1. Comparative analysis of the conceptual DFT indices of the reagents

The global indices, namely, the electronic chemical potential, μ, chemical hardness, η, electrophilicity, w, and nucleophilicity, N, of the reagents involved in these addition reactions are given in Table 1.

Table 1 DFT/B3LYP/6-31(d) chemical hardness, electronic chemical potential, electrophilicity and nucleophilicity in eV, of the α-himachalene, 3,7-dichlorohimachalane and HCl acid

Molecule	**η**	**μ**	**ω**	**N**
α-himachalene	6.64	-2.74	0.56	3.45
6-chloro-α-himachalene	6.99	-3.07	0.67	2.95
HCl	9.39	-4.32	0.99	0.50

The electronic chemical potential of α-himachalene and 3,7-dichlorohimachalane, -2.74 and -3.07 eV respectively are slightly higher than that of HCl -4.32 eV. Thus, the α-himachalene and 3,7-dichlorohimachalane will have a tendency to exchange electron density with the HCl along these addition reactions, suggesting non-polar reactions.

α-himachalene and 3,7-dichlorohimachalane, presents an electrophilicity w index of 0.56, 0.67 eV and a nucleophilicity N index of 3.45, 2.95 eV respectively, being classified as a moderate electrophile and as a strong nucleophile according to the electrophilicity54 and nucleophilicity55 scales. Note that HCl presents an electrophilicity w index of 0.99 eV and a nucleophilicity N index of 0.50 eV, HCl will participating in these reactions as electrophilic derivative.

4.1. An analysis of the reactivity local indices of the reagents

By approaching a non-symmetric electrophilic/nucleophilic pair along a polar or ionic process, the most favourable reactive channel is that associated with the initial two-center interaction between the most electrophilic center of the electrophile and the most nucleophilic center of the nucleophile. Recently, Domingo proposed the nucleophilic P_k^- and electrophilic P_k^+ Parr functions, derived from the changes of spin electron-density.

Accordingly, the HOMO, LUMO, Electrostatic potential maps, nucleophilic P_k^- and electrophilic P_k^+ Parr functions centers of the reagents involved in this addition reaction (see Fig. 2).

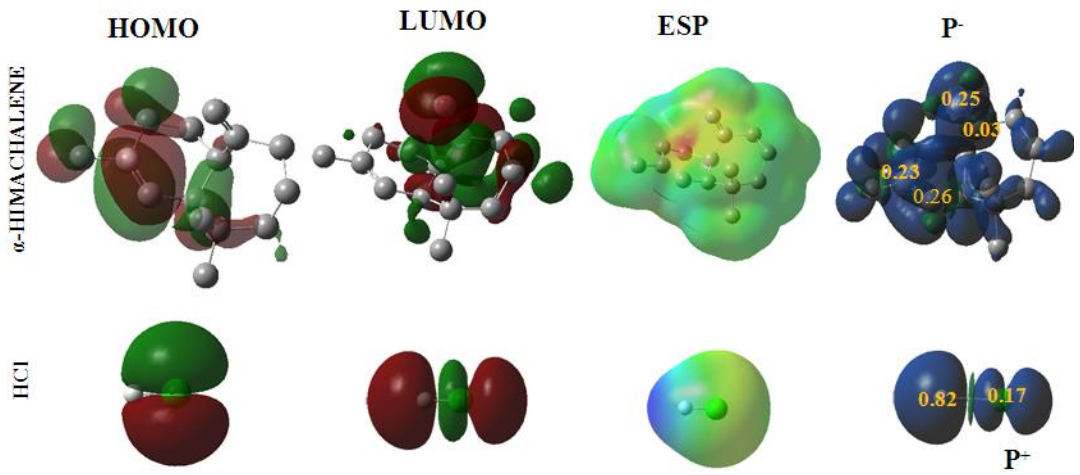

Fig. 1. the HOMO, LUMO, Electrostatic potential maps, nucleophilic P_k^- and electrophilic P_k^+ Parr functions

Therefore, it is predictable that the most favourable electrophile–nucleophile interaction along the nucleophilic attack of α-himachalene on HCl acid in a polar process will take place between the most nucleophilic center of α-himachalene, the C2 carbon atom, and the most electrophilic center of HCl, the H hydrogen atom. We also note that the HOMO orbital of α-himachalene is totally localized on the C2 = C3 double bond, which shows that the attack of one mole of chloridhyric acid is regiospecifically on this double bond. This prediction is in complete agreement with the experimental observations.

4.3. Study of the reaction paths associated with the addition reaction of α-himachalene with HCl

Due to the non-symmetry of the two reagents, the addition reaction of α-himachalene and 3,7-dichlorohimachalane with HCl can take place along four isomeric channels: one pair of stereoisomeric channels and one pair of regioisomeric ones (figure 3). In this part we want to study the stereoselectivity observed experimentally.

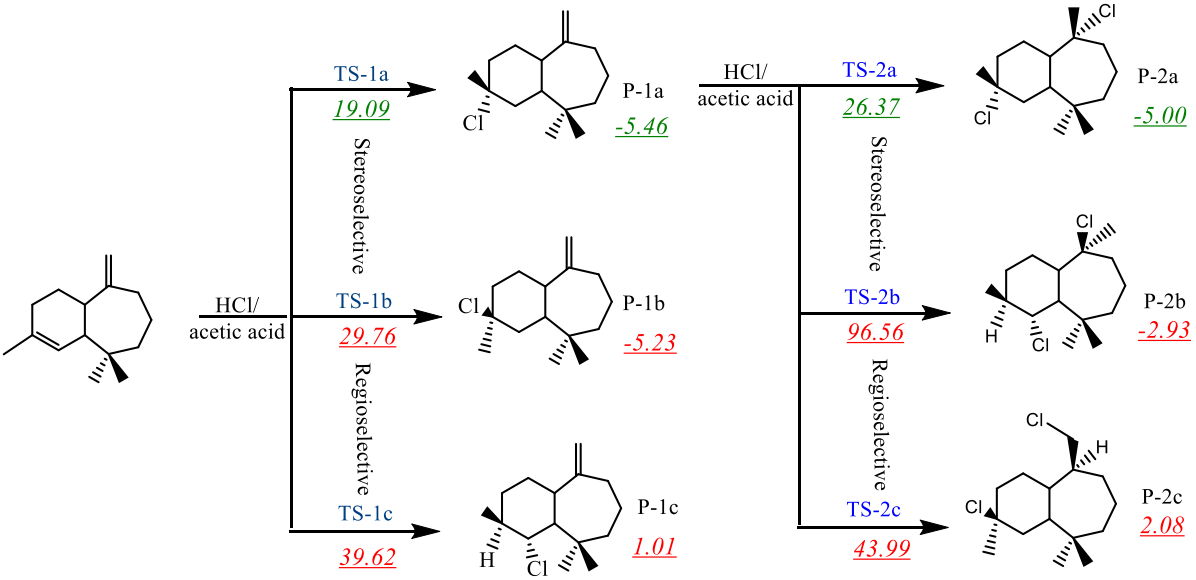

Fig. 3. The competitive reactive channels associated with the addition reaction of α-himachalene and 3,7-dichlorohimachalane with HCl. B3LYP/6-31G(d) relative energies, are given in kcal mol^{-1}.

The activation energies associated with the competitive channels are 19.09 (TS1a), 29.76 (TS1b), 39.62 (TS1c), 26.37 (TS2a), 96.56 (TS2b) and 43.99 (TS2c) kcal mol-1. Some appealing conclusions can be drawn from these relative energies: (i) the activation energy associated with the addition reaction of α-himachalene with HCl via TS1a is 19.09 kcal mol^{-1} lower in energy than TS1b (29.76) and TS1c (39.62), (ii)the activation energy associated with the addition reaction of 3,7-dichlorohimachalane with HCl via TS2a is 26.37 kcal mol^{-1} lower in energy than TS2b (96.56) and TS2c (43.99) indicating that the formation of the product P1a and P1a are kinetically very favored.

(ii) These addition reactions are exergonic by 5.23 and 2.93 kcal mol^{-1} (P1b and P2b). Note that the most favourable reactive channel associated with the addition reaction involving the P1a and P2a are exergonic by only 5.46 and 5.00 kcal mol^{-1}, the formation of the product P1c and P2c is endothermic by 1.01 and 2.08 kcal mol^{-1}, consequently, the products P1a and P2a do not only kinetically favored but also the thermodynamically in good agreement with experimental observations.

Optimized TSs involved in the addition reactions between of α-himachalene and 3,7-dichlorohimachalane with HCl, including some selected distances, are given in Figure 4.

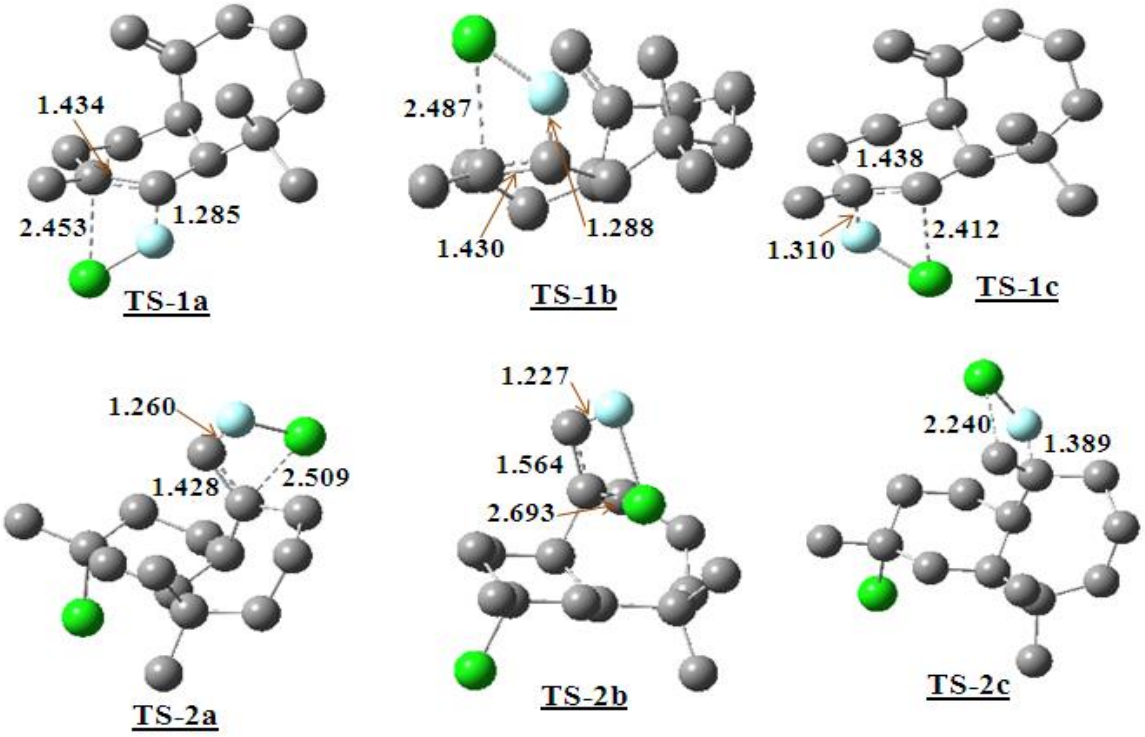

Fig. 4. B3LYP/6-31G(d) optimized geometries of the TSs involved in the addition reactions between α-himachalene and 3,7-dichlorohimachalane with HCl. Distances are given in Angstroms.

At the TSs associated with the addition reaction between α-himachalene and HCl, the distances between the atoms involved in the formation of the C–Cl and C–H single bonds are: 2.453 °A (C3–Cl) and 1.285 °A (H–C2) at TS1a, 1.288 °A (H–C2) and 2.487 °A (C3–Cl) at TS1b and 1.310 °A (H–C3) and 2.412 °A (C2–Cl) at TS1c.

At the TSs associated with the addition reaction between 3,7-dichlorohimachalane and HCl, the distances between the atoms involved in the formation of the C–Cl and C–H single bonds are: 2.509 °A (C7–Cl) and 1.260 °A (H–C13) at TS2a, 1.227 °A (H–C2) and 2.693 °A (C7–Cl) at TS2b and 1.389 °A (H–C73) and 2.240 °A (C13–Cl) at TS2c. Consequently, the products P1a and P2a are favored.

To better understand the reaction mechanism of this addition reaction, we chose some points on IRC for the analyst's figure 5.

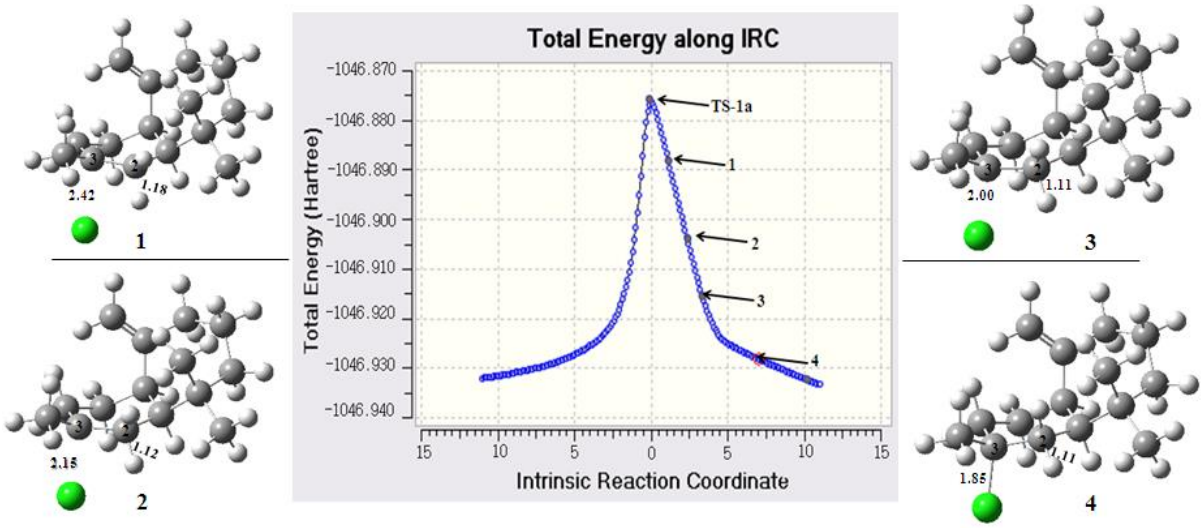

Fig. 5. The IRC profile of the favorable TS-1a together with the position of the selected points of the addition reaction between α-himachalene and HCl

At P1, which is the first point after TS-1a, where the inter-atomic distances between C2-H and C3-Cl are 1.18 Å and 2.42 Å respectively, in this product, the double bond is not disappeared and the simple bonds not formed yet, in the product P2 the lengths of bonds C2-H and C3-Cl are 1.12 Å and 2.15 Å, and firstly the single bond C2-H was formed. In the product P3 the chlorine atom approaches the C3 carbon atom and the bond between the two atoms is not formed, in product P4 the C3-Cl bond is formed on the α-side, therefore the molecular mechanism of HCl addition on α-himachlene is non-concerted.

5. Conclusion

2,5-Dichloro-2,5,9,9-tetramethyl-decahydro-benzocycloheptene has been synthesized using addition Reactions between α-himachalene and HCl, our experimental results shows that this reaction is regio- and stereospecific. To understand the mechanism and regio- and stereospecificity, this reaction have been theoretically studied using DFT methods at the B3LYP/6–31G(d) level of theory. The reactive channels corresponded to the regioselective and stereoselective approach modes have been explored and characterized. We can summarize the results of the present study in the following points:

The relatively low activation energies found for both addition reaction are explain by the high nucleophilic nature of both α-himachalene and 3,7-dichlorohimachalane, and the moderate electrophilic nature of HCl, giving a good explanation of the experimental conditions of these addition reaction.

Analysis of the computed nucleophilic Parr functions of the nucleophilic ethylenes α-himachalene and 3,7-dichlorohimachalane, as well as electrophilic Parr functions of the electrophilic HCl justifying the regioselectivity and stereoselectivity obtained experimentally.

References

Arnal-Schnebelen et al., 2004 – *Arnal-Schnebelen B. Hadji-Minaglou F., Peroteau J-F., Ribeyre F., Billerbeck V.G.* (2004). Essential oils in infectious gynaecological disease: a statistical study of 658 cases, *International Journal of Aromatherapy*, 14: 192-197.

Becke, 1993 – *Becke A.D.* (1993). A new mixing of Hartree-Fock and local density-functional theories, *J. Chem. Phys.*, 98; 1372–137.

Domingo et al., 2008 – *Domingo L. R., Chamorro E., Pérez P.* (2008). Understanding the Reactivity of Captodative Ethylenes in Polar Cycloaddition Reactions. A Theoretical Study, *J. Org. Chem.* 73, 4615-4624.

El Haib et al., 2018 – El Haib A., Elajlaoui R., El Idrissi M., Moumou M., Abouricha S., Zeroual A., Benharref A., El Hajbi A. (2018) "The mechanism, the chemoselectivity and the

regioselectivity of the 1-Benzyl-4-ethynyl-1H-[1,2,3]triazole and 1-Azidomethyl-4-tert-butyl-benzene in [3+2] cycloaddition reactions: a DFT study", *Mor. J. Chem.* 6, (1), 14-21.

El Idrissi et al., 2016 – *El Idrissi, M., El Haib, A., Zoubir, M., Hammal, R., Zeroual, A., EL Hajbi, A.* (2016). Understanding the regioselectivite of the Baeyer-Villiger reaction of bicyclo[4.2.0]octan-7-one and bicyclo[3.2.0]heptan-6-one: A DFT Study, *Journal of Computational Methods in Molecular Design,* 6: 75-79.

El Idrissi et al., 2017 – *El idrissi M., El Ajlaoui R., Zoubir M., Abouricha S., Moumou M., Ourhriss N., Zeroual A., Benharref A., El Hajbi A.* 2017. Theoretical study of the chemo- and regioselectivity toward [3+2] cycloaddition reaction between mesitonitrile oxides and 2-fluoren-9-ylidene-malononitrile, *Journal of Materials and Environmental Sciences*, 8 (10), 3564-3569.

Fukui, 1970 – *Fukui K.* (1970). Formulation of the reaction coordinate, *J. Phys. Chem.* 74, 4161–4163.

Kurkin, 2003 – *Kurkin V.A.* (2003) phenylpropanoids from medicinal plants: distribution, classification, structural analysis, and biological activity, *Chemistry of Natural Compounds*, 39: 123–153.

Mangena et al., 1999 – *Mangena T., Muyima N.Y.O.* (1999). Comparative evaluation of the antimicrobial activities of essential oils of Artemisia afra, Pteronia incana and Rosmarinus officinalis on selected bacteria and yeast strains, *Lett. Appli. Microbiol. 28:* 291-296.

Nacereddine et al., 2015 – *Nacereddine A.K., Sobhi C., Djerourou A., Ríos-Gutiéerrez M., Domingo L. R.* (2015) Non-classical CH O hydrogen-bond determining the regio- and stereoselectivity in the [3 + 2] cycloaddition reaction of (Z)-C-phenyl-N-methylnitrone with dimethyl 2-benzylidenecyclopropane-1,1-dicarboxylate. A topological electron-density study, RSC Adv. 5; 99299–99311.

Ourhriss et al., 2017 – *Ourhriss, N., Zeroual, A., Ait Elhad, M., Mazoir, N., Abourriche, A., Gadhi, C. A., Benharref, A., El Hajbi*, A. (2017). Synthesis of 1-isopropyl-4,7-dimethyl-3-nitronaphthalene: An experimental and theoretical study of regiospecific nitration, *Journal of Materials and Environmental Sciences,* 8 (4): 1385-1390.

Parr et al 2009 – *Parr, R. G., Szentpaly, L. V., Liu, S.* (1999). Electrophilicity Index, *J Am ChemSoc,* 121: 1922-1924.

Rassolov et al 2001 – *Rassolov V. A., Ratner M. A., Pople J. A., Redfern P. C., and Curtiss L. A.* (2001). 6-31G* Basis Set for Third-Row Atoms, *J. Comp. Chem.*, 22: 976-84.

Schlegel, 1982 – *Schlegel H.B.* (1982). Optimization of Equilibrium Geometries and Transition. Structures, J. *Comput. Chem.*, 2, 214-218.

Sivropoulou et al., 1996– *Sivropoulou A., Papanikolaou E., Nikolaou C., Kokkini S., Lanaras T., Arsenakis M.* (1996) Antimicrobial and Cytotoxic Activities of Origanum Essential Oils, *J. Agric. Food Chem.* 44: 1202-1205.

Zambonelli et al., 2004– *Zambonelli A., D'Aurelio A.Z., Severi A., Benvenuti E., Maggi L., Bianchi A.,* (2004). Chemical Composition and Fungicidal Activity of Commercial Essential Oils of Thymus vulgaris L., *J. Essent. Oil Res.*, 16: 69-47.

Zeroual et al., 2015 – *Zeroual, A., Benharref, A., El Hajbi, A.* (2015). Theoretical study of stereoselectivity of the [1+2] cycloaddition reaction between (1S,3R,8S)-2,2-dichloro-3,7,7,10-tetramethyltricyclo[6,4,0,01.3]dodec-9-ene and dibromocarbene using density functional theory (DFT) B3LYP/6-31G*(d), *J Mol Model,* 21: 1610-2940.

Zeroual et al., 2015– *Zeroual, A., El Haib, A., Benharref, A., El Hajbi A.* (2015). A combined experimental and theoretical study of highly chemioselectivity acetylation of diterpene, *Journal of Computational Methods in Molecular Design,* 5: 58-62.

Zeroual et al., 2015 – *Zeroual, A., Zoubir, M., Hammal, R., Benharref, A., El Hajbi, A.* (2015). Understanding the regioselectivity and reactivity of Friedel–Crafts benzoylation using Parr functions, *Mor. J. Chem*, 3: 356-360.

Zeroual et al., 2017 – *Zeroual A., El Idrissi M., El Ajlaoui R., Ourhriss N., Abouricha S., Mazoir N., Benharref A., El Hajbi A.* (2017). MEDT Study of the Mechanism and Regioselectivity of Diazocompounds and Alkenes in [3+2] Cycloaddition Reaction, *European Journal of Molecular Biotechnology*, 5(1), 43-49.

Zeroual et al., 2017 – *Zeroual A., El Idrissi M., Zoubir M., El Ajlaoui R., Abouricha S., El Hajbi A.* (2017). Theoretical Study of the Mechanism and Regioselectivity of Prop-2-Yn-1-Ol with

Azide in [3+2] Cycloaddition Reactions, *Open Access Journal of Translational Medicine & Research*, 1(1), 1-5.

Zeroual et al., 2017 – *Zeroual A., Zoubir M., El Idrissi M., El ajlaoui R., El Haib A., Abouricha S., Mazoir N., El Hajbi A.* (2017). Theoretical Analysis of Reactivity and Regioselectivity in [1+2] Cycloaddtion Reaction of Some Monoterpenes with Dichlorocarbene, *Global Journal of Science Frontier Research: B Chemistry*, 17 (1) Version 1.0.

Zhang et al., 2015 – *Zhang B., White J. M., David J.* (2015). Regioselective synthesis of fullerene multiadducts via tether-directed 1,3-dipolar cycloaddition, *Org. Biomol. Chem*. 13, 10505-10510.

Zoubir et al., 2016 – *Zoubir M., Zeroual A., Benharref A., El Hajbi A.* (2016). Understanding the Holleman Rule in the Electrophilic Substitution Reaction Using Parr Functions, *Journal of Computational Methods in Molecular Design*, 6 (4), 1-4.

Zoubir et al., 2017 – *Zoubir M., Zeroual A., El Idrissi M., Bkiri F., Benharref A., Mazoir N., El Hajbi A.* (2017). Experimental and theoretical analysis of the reactivity and regioselectivity in esterification reactions of diterpenes (totaradiol, totaratriol, hinikione and totarolone), *Mediterranean Journal of Chemistry*, 6(4), 98-107.

Zoubir et al., 2017 – *Zoubir M., Zeroual A., El Idrissi M., El Haib A., Moumou M., Hammal R., Mazoir N., Benharref A., El Hajbi A.* (2017). Understanding the Chemoselectivity and Stereoselectivity in Michael Addition Reactions of β-Hydroxyparthenolides and Amines such as Pyrrolidine, Morpholine, Piperidine and 1-Methylpiperazine: a DFT Study, *Journal of Materials and Environmental Sciences*, 8 (3), 990-996.

Zoubir et al., 2017 – *Zoubir M., El Idrissi M., El Ajlaoui R., El Haib A., Abouricha S., Zeroual A., Benharref A., El Hajbi A.* (2017). Theoretical Investigation of the Chemo and the Regioselectivity of the Reaction Oxidation of Bicyclo[3.2.0]Hept-2-En-6-One by Hydrogen Peroxid, *European Reviews of Chemical Research,* 4(1), 28-33.

Published in the Slovak Republic
European Reviews of Chemical Research
Has been issued since 2014.
E-ISSN: 2413-7243
2018, 5(1): 30-39

DOI: 10.13187/ercr.2018.1.30
www.ejournal14.com

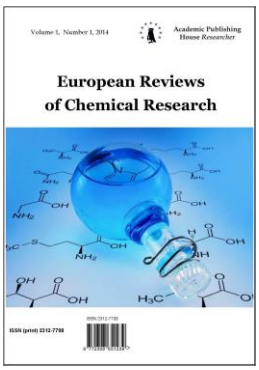

Novel Polyheterocyclic Cyanine Dyes: Synthesis, Photosensitiztion and Solvent/Electronic Transitions Correlation

H.A. Shindy [a, *]

[a] Department of Chemistry, Faculty of Science, Aswan University, Aswan 81528, Egypt

Abstract

Novel polyheterocyclic cyanine dyes covering aza-cyanine dyes and bis aza-cyanine dyes derived from 3,8-diethyl-2,7-diphenyl benzo [2,3-b; 2̄,3̄-b̄] bis furo[3,2-d] pyrazolium iodide quaternary salt were prepared. The electronic visible absorption spectra for all the synthesized cyanines were investigated in 95 % ethanol solution to evaluate their photosensitization/electronic transitions correlation. The cyanine dyes were thought to be better photosensitizers when they absorb the visible light to initiate the electronic transitions at higher wavelength bands (bathochromic shifted and/or red shifted dyes). Consequently, the photosensitization of the cyanine dyes decreases when they absorb the visible light to initiate the electronic transitions at lower wavelength bands (hypsochromic shifted and/or blue shifted dyes). Solvent/electronic transitions correlation study for some selected cyanine dyes were carried out in pure solvents having different polarities [water (78.54), Dimethylformamide (36.70), ethanol (24.3), chloroform (4.806), benzene (2.28) and dioxane (2.209)] to evaluate their solute/solvent interaction properties (general and/or specific solvent effects). Structural identification were confirmed using elemental analysis, visible spectra, IR and ^{1}H NMR spectral data.

Keywords: cyanine dyes, aza-cyanine dyes, synthesis, photosensitization/electronic transitions correlation, visible spectra, solvent / electronic transitions correlation.

1. Introduction

Cyanine dyes (Shindy, 2017; Shindy, 2016; Shindy, 2018; Shindy et al., 2017; Shindy et al., 2017a; Solomon et al., 2014; Lynch et al., 2013; Shindy et al., 2012; Arjona et al., 2016; Shindy et al., 2015; Shindy, 2015; Shindy, Koraiem, 2008) have a wide range and various applications in different fields of science and technology. Their uses and applications include but not limited to spectral sensitizers for silver halide emulsions in photographic material industry for coloured and non coloured (black and white) films (cyanine dyes were originally used, and still are, to increase the sensitivity range of photographic emulsions, i. e. to increase the range of wavelengths which will form an image on the film) (Msaki, Tadashi, 1992; Mari, 1993; Tadashi, 1992; Nobuaki, 1995; Yoshio, Tadahire, 1999), as tools for lasers (Toshiyoshi et al., 2003; Tsutomu et al., 1994), as optical recording media (Toshio, 1992), optical filters (Hiroshi, 1999), optical information recording disk (Katsuji, Katsuhiko, 1991), as inks containing near-IR absorber for optically readable printing (Rivera et al., 2007), and for the development of integrated optochemical sensors

* Corresponding author
E-mail addresses: hashindy2@hotmail.com (H.A. Shindy)

(Clegg et al., 1992). In addition, cyanine dyes can also be very usefully employed for conformational studies via fluorescence energy transfer (Norman et al., 2000; Mortensen, Chui, 2002), agarose gel and capillary electrophoresis staining (Zhu et al., 1994), DNA analysis in polymerization chain reactions (Schwartz, Ulfelder, 1992; Bengtsson et al., 2003) and flow cytometry (Hirons et al., 1994), or as fluorescent probes for membrane fluidity (Kurihara et al., 1977; Armitage, O'Brien, 1992) and membrane potential studies (Reers et al., 1991) and as a probe for albumin and collagen in the extracellular matrix (Panova et al., 2007). Recently, cyanine dyes have been tested for therapeutic uses, and in the future time cyanine dyes may find very important applications in this field.

Taking in account and consideration these important, useful and interested applications of cyanine dyes, we prepared here new classes of photosensitizers and solvatochromic aza-cyanine dyes as new synthesis contribution and spectroscopic investigation in this field, and hoping that it may be find useful uses in any of the wide fields and various aspects of cyanine dyes applications, particularly as photosensitizers in photographic material industry for colored and non colored (black and white) films, as acid-base indicators in analytical chemistry, as probes for determining solvent polarity in solution chemistry and /or as anti-bacterial strains (bactericidals), anti-fungi strains (fungicidals) in pharmaceutical (pharmacological) industry.

2-Results and Discussion

2.1. Synthesis

Reaction of 3,8-diethyl-4,9-dimethyl -benzo [2,3-b; 2̄,3̄-b̄] bis furo[3,2-d] pyrazolium iodide quaternary salt (1) (Shindy, 2007) with equimolar ratios of the nitroso compounds (ρ.nitroso-phenol, α-nitroso-β-naphthol, β-nitroso-α-naphthol) in ethanol as organic solvent and piperidine as a basic catalyst achieved the 4[2(1)]-aza-cyanine dyes (2a–c), Scheme (1).

In addition, reaction of 1 M ratios of the diquaternizsed compound (1) with 2 M ratios of the nitroso compounds (4-nitroso-phenol, 1-nitroso-2-naphthol, 2-nitroso-1-naphthol) in ethanol and in presence of few mls of piperidine resulted the 4,9 [2(1)]-bis aza-caynine dyes (3a-c), Scheme (1).

Chemical confirmations takes place through reaction of the 4[2(1)]-aza-cyanine dyes (2a-c) with equimolar ratios of the same nitroso compounds (ρ.nitroso-phenol, α-nitroso-β-naphthol, β-nitroso-α-naphthol) in ethanol catalyzed by piperidine to produce the same 4,9 [2(1)]- bis aza-cyanine dyes (3a–c), characterized by melting points, mixed melting points, same IR and ^{1}H NMR spectral data, Method (2), Scheme (1).

The structure of the prepared compounds was identified by elemental analysis (Table 1), visible spectra (Table 1) as well as IR (Wade, 1999) (Table 2) and ^{1}H NMR (Wade, 1999a) (Table 2) spectral data.

2.2. Synthesis mechanisms

The synthesis mechanism of the aza-cyanine dyes (2a-c) is suggested to proceeds as follows:

1-The first step in this mechanism involves the formation of the carbanion ion (a) via attacking of the basic catalyst piperidine to the active acidic methyl group of the heterocyclic quaternary salt, Scheme (2).

2-The second step involves nucleophilic attack of the carbanion ion (a) to the positively center of the ionized nitroso group to form the anion (b), Scheme (2).

3-The third step represents transfer of a proton from piperidine$^+$-H to the anion (b) yielding the intermediate compound (c), Scheme (2).

4-The fourth step involves the dehydration of the intermediate compound (c) by the action of piperidine and heating to form the required aza-cyanine dyes (d), Scheme (2).

The synthesis mechanism of the bis aza-cyanine dyes (3a-c) is suggested to proceeds in a way similar to that of the aza-cyanine dyes (2a-c).

2.3. Photosensitization / electronic transitions correlation

Photosensitization/electronic transitions correlation for all the synthesized cyanine dyes was carried out through examining their electronic visible absorption spectra in 95 % ethanol solution. The cyanine dyes were thought to be better photosensitizers when they absorb the visible light to initiate the electronic transitions at higher wavelength bands (bathochromic shifted and/or red shifted dyes). Consequently, the photosensitization of the cyanine dyes decreases when they absorb the visible light to initiate the electronic transitions at lower wavelength bands (hypsochromic shifted and/or blue shifted dyes) (Shindy et al., 2002; Shindy et al., 2006; Shindy et al., 2015a;

Shindy et al., 2015b). So, we may say that the photosensitization of one cyanine dye is higher than the other one if the wavelength of the maximum absorption spectrum of the former one is longer than that of the latter one. In contrary, we may say that the photosensitization of one cyanine dye is lower than the other one if the wavelength of the maximum absorption spectrum of the former one is shorter than that of the latter one. Studying the electronic visible spectra of cyanine dyes in 95 % ethanol solution is very important in the case of cyanine dyes because the extensive uses of these dyes as photographic sensitizers for silver halide emulsion in photosensitive material industry.

The visible electronic transitions spectra of the aza-cyanne (bis aza-cyanine) dyes 2a–c (3a–c) in 95 % ethanol solution discloses bands in the region 390–485 nm (405–500 nm), which their positions and molar extinction coefficients are influenced by the type of the substituents (X), the number of the electronic charge transfer pathways inside the dyes molecules, the number of the aza-methine units in the dyes structures and by the nature of the planarity of the dyes, Schemes (1), (3), Table (1).

So, substituting X = 4-OH by X = 2-OH, 5,6-benz and/or 2-OH, 3,4-benz passing from phenol dyes 2a (3a) to naphthol dyes 2b,c (3b,c) imparted bathochromic shifts in addition to increasing the intensity of the bands. This can be attributed to increasing conjugation in the latter dyes due to the presence of the more π–delocalization naphthalene nucleus compared by the less π–delocalization benzene nucleus in the former dyes, Scheme (1), Table (1).

In addition, substituting X = 2-OH, 5,6-benz in β-naphthol dyes 2b (3b) by X = 2-OH, 3,4-benz to obtain α-naphthol dyes 2c (3c) resulted in red shifted and intensified absorption bands, Scheme (1), Table (1). These may be related to the higher planarity of the latter dyes which leads to easier mobility of the electronic charge transfer pathways to the positively charged heterocyclic pyrazolium iodide quaternary salts residue and consequently red shift occurs, Scheme (1), Table (1).

Besides, comparing the electronic visible absorption spectra of aza-cyanine dyes (2a–c) by their analogous bis aza-cyanine dyes (3a–c) reveals that the latter dyes possesses bathochromic shifted and intensified bands compared with the former dyes, Scheme (1), Table (1). This can be related to the following two factors: a-The presence of two electronic charge transfer pathways in the latter dyes (3a-c) in correspondence to one electronic charge transfer pathways in the former dyes (2a-c), Scheme (3). b-Increasing conjugation due to increasing the number of the aza-methine (-CH=N-) groups in the latter dyes (3a-c) compared to the former dyes (2a-c) by one aza-methine unit, Scheme (1).

2.4. Solvent/electronic transitions correlation:

Visible electronic transitions study in pure solvents having different polarities is very important in the case of cyanine dyes in order to select the best solvents to use of these dyes as photosensitizers when they are applied as photographic sensitizers in photographic material industry. In addition, this study bears to have a great practical importance in the case of cyanine dyes because the extensive uses of these dyes in the textile industry (Gaspar et al., 2008) and/or as probes for determining solvent polarity in physical, physical organic and/or solution chemistry (Green et al., 1992).

The visible electronic transitions spectra of the aza-cyanine dye.(2a) and the bis aza-cyanine dye (3a) in pure solvents of different dielectric constant viz water (78.54), DMF (36.70), ethanol (24.3), chloroform (4.806), benzene (2.28) and dioxane (2.209) (Shindy et al., 2012; Shindy, 2007) are recorded. The λ_{max} and ε_{max} values of the absorption bands due to different electronic transitions within the solute molecule in these solvents are represented in Table (3).

From Table (3), it's clearly that the visible electronic transition absorption spectra of the dyes in ethanolic medium are characterized by the presence of three essential absorption bands. These bands can be assigned to intermolecular charge transfer transitions (Shindy et al., 2012; Shindy, 2007). These charge transfer is due to transfer of lone pair of electrons from the phenolic hydroxyl oxygen atom (the electron donating and/or the basic center of the dyes) to the positively charged heterocyclic pyrazolium iodide quaternary salts residue (the electron accepting and/or the acidic center of the dyes) and vice versa, Scheme (3).

Careful examination of the results in Table (3) shows that, changing the solvent from ethanol to DMF caused a bathochromic shifts for the absorption bands of the dyes accompanied with increasing the intensity of the bands. This can be attributed to increasing the polarity of the solvent

due to increasing the dielectric constant of DMF related to ethanol (general solvent effects and/or positive solvatochromism).

In addition, replacing the solvent of ethanol by chloroform, benzene and/or dioxane solvents reveals red shifted and intensified absorption bands for the dyes, Table (3). This can be related to solute–solvent interaction through intermolecular hydrogen bond formation between ethanol and the lone pair electrons of phenolic hydroxy oxygen atom (specific solvent effects and/or negative solvatochromism), Scheme (4). This decreases slightly the electron density on the phenolic hydroxy oxygen atom (the electron rich and/or the basic center of the dyes), and consequently decreases to some extent the mobility of the attached π-electrons over the conjugated system pathways to the positively charged heterocyclic pyrazolium iodide quaternary salts residue (the electron poor and/or the acidic center of the dyes), and so blue shifts occurs in ethanol related to chloroform, benzene and dioxane, Scheme (4).

Besides, it's was observed that the electronic visible absorption spectra bands of the dyes in: a-$CHCl_3$ reveals bathochromic shifted and intensified bands compared with their spectra bands in benzene and dioxane, Table (3). b-Benzene gives red shifted with increasing the intensity of the bands if compared with their spectra bands in dioxane, Table (3). This can be related to increasing the polarity of the solvents due to increasing the dielectric constants in the order of $CHCl_3$ > benzene > dioxane (general solvent effects and/or positive solvatochromism), Table (3).

Furthermore, it's also interest to notice that, the electronic visible absorption spectra of the dyes in water relative to the other solvents reveals a hypsochromic shifts for the absorption bands in addition to decreasing the number and intensity of the bands, Table (3). This can be ascribed to the possible interaction of water molecules with the lone pair electrons of the phenolic hydroxyl oxygen atom via formation of intermolecular hydrogen bonding (specific solvent effects and/or negative solvatochromism), Scheme (4). This makes difficult the transfer of the electronic charge from the phenolic hydroxyl oxygen atom (the electron releasing and/or the basic center of the dyes), to the heterocyclic pyrazolium iodide quaternary salts residue (the electron attracting and/or the acidic center of the dyes), and accordingly blue shifts occur in water related to other solvents, Table (3).

3. Conclusion

From this study it could be concluded that:

1. The higher photosensitization and/or the visible electronic transitions (longer wavelength bands and/or bathochromic shifted bands) of all the synthesized cyanine dyes in 95 % ethanol solution and/or in pure solvents of different polarities for some selected synthesized cyanine dyes increase by:

a. Increasing π–delocalization conjugation in the dyes molecules in the order of: naphthyl cyanine dyes > phenyl cyanine dyes in the sequence: α-naphthol and β-naphthol cyanine dyes > phenol cyanine dyes.

b. Increasing planarity of the dyes molecules in the order of: higher planarity cyanine dyes > lower planarity cyanine dyes in the sequence: α-naphthol cyanine dyes > β-naphthol cyanine dyes.

c. Increasing number of the electronic charge transfer pathways inside the dyes molecules in the order of: two electronic charge transfer pathways cyanine dyes > one electronic charge transfer pathways cyanine dyes in the sequence: bis aza-methine cyanine dyes > aza-methine cyanine dyes.

d. Increasing conjugation in the dyes molecules due to increasing the number of the aza-methine (-CH=N-) units in the dyes structures in the order of: bis aza-methine cyanine dyes > aza-methine cyanine dyes.

e. Increasing dielectric constant and/or polarity of the solvents in the order of: higher polarity solvents > lower polarity solvents in the sequence: i-DMF > EtOH, $CHCl_3$, Benzene and Dioxane. ii-$CHCl_3$ > Benzen and Dioxane. iii-Benzene > Dioxane.

f. Absence of Hydrogen bonding and/or molecular complex formation between the solvent and the solute (cyanine dyes molecules) in the order of: no hydrogen bond formation solvents > hydrogen bond formation solvents in the sequence: i-EtOH < $CHCl_3$, Benzene and Dioxane. ii-H_2O < DMF, EtOH, $CHCl_3$, Benzene and Dioxane.

2. The intensity of the colours and/or the electronic charge transfer pathways of the aza-cyanine dyes (2a-c) and the bis aza-cyanine dyes (3a-c) can be illustrated in the light of the

suggested two mesomeric electronic transitions structures, producing a delocalized positive charge over the conjugated chromophoric group system of the dyes, Scheme (3).

3. Because cyanine dyes have multi purposes uses and applications in various fields and different research area, this research paper is recommended not only for heterocyclic and/or cyanine dyes chemists but also for other scientists in other fields like biology, biotechnology, biochemistry, physics, engineering, pharmacology and, medicine. Also, this research paper is recommended for all whom interested in the light absorbing systems in their research, labeling of biomolecules and/or in the synthesis and characterization of complex organic compounds.

4. Expermental

4.1. General

All melting points are uncorrected. Elemental analyses were carried out at the Microanalytical Center of Cairo University (Cairo, Egypt) by an automatic analyzer (Heraeus). IR (KBr pellets) spectra were determined on a Perkin Elmer Infrared 127 spectrophotometer (Cairo University). ^{1}H NMR spectra were obtained using a varian Gemini NMR spectra 300 MHz spectrometers (Cairo University). Electronic visible absorption spectra were carried out on UV spectrophotometer (Department of Chemistry, Faculty of Science, Aswan University, Aswan, Egypt).

4.2. Synthesis

4.2.1-Synthesis of 3,8-diethyl-9-methyl-2,7-diphenyl-5,10-dione-benzo [2,3-b; 2̄,3̄-b̄] bis furo [3,2-d] pyrazolium iodid quaternary salt-4[2(1)]-aza-cyanine dyes (2a–c):

An equimolar ratios (0.01 mole) of the quaternary salt (1) and nitroso compounds (ρ.nitroso phenol, α-nitroso-β-naphthol, β-nitroso-α-naphthol) were heated under reflux for 6-8 hours in ethanol (30 ml) and presence of piperidine (1-2 ml). The reaction mixture which attained from brown to deep brown colours at the end of refluxing were filtered while hot, concentrated, cooled and acidified by glacial acetic acid. The precipitates which appear by adding of cold water were filtered off, washed several times with water, air dried and crystallized from ethanol. The results were listed in Table (1).

4.2.2-Synthesis of 3,8-diethyl-2,7-diphenyl-5,10-dione-benzo [2,3-b; 2̄,3̄-b] bis furo [3,2-d] pyrazolium iodid quaternary salt-4,9[2(1)]-bis aza-cyanine dyes (3a–c):

Two different Methods were used to synthesize these cyanines:

Method (1): A mixture of 1 : 2 M ratios of (1) and nitroso compounds (ρ.nitroso phenol, α-nitroso-β-naphthol, β-nitroso-α-naphthol) were allowed to boil under reflux for 6-8 hours in ethanol (30 ml) containing piperidine (1-2 ml). The reaction mixture which attained from brown to deep brown colours at the end of refluxing were filtered off while hot, concentrated, cooled and acidified by glacial acetic acid. The precipitates were collected and crystallized from ethanol. The results were summarized in Table (1).

Method (2): An equimolar ratios (0.01 mole) of the aza-cyanine dyes (2a–c) and nitroso compounds (ρ.nitroso phenol, α-nitroso-β-naphthol, β-nitroso-α-naphthol) were dissolved in ethanol (30 ml), then piperidine (1-2 ml) was added. The reaction mixture was allowed to heat under reflux for about 6-8 hours and attained a permanent brown to deep brown colours at the end of refluxing. It was filtered while hot, concentrated, cooled and acidified by acetic acid. The precipitated products which separated by water were collected and crystallized from ethanol to give the same bis aza-cyanine dyes (3a–c) obtained by Method 1. See Table (1).

4.3. Photosensitization and solvent / electronic transitions correlation:

The organic solvents were of spectroscopic grade or were purified according to recommended methods (Shindy et. al., 2012; Shindy, 2007). The electronic visible absorption spectra of the dyes were recorded on UV-VIS recording spectrophotometer using 1 cm quartz cells. The stock solution were about $1x10^{-3}$ m. Lower molarities were obtained by an accurate dilutions. The spectra were recoded immediately to eliminate as much as possible the effect of time.

5. Current future developments

The current and the future research developments aim to provide novel synthetic methods for the preparation of different classes of highly antimicrobial active, Anti-tumor, p-H sensitive, highly photographic sensitizers, non toxic, high stability, light fastness, near IR (Infrared), fluorescent, anti corrosion, strong labeled DNA and extra conjugated cyanine dyes. Such as oxadiazine cyanine dyes, thiazole cyanine dyes, metal stabilized cyanine dyes, pentamethine cyanine dyes, hexamethine cyanine dyes, heptamethine cyanine dyes, octamethine cyanine dyes, nonamethine cyanine dyes, undecamethine cyanine dyes and tridecamethine cyanine dyes.

6. Conflict of interest

There is no conflict of interest.

7. Acknowledgement

I am thankful to the Chemistry department, Faculty of Science, Aswan University, Aswan, Egypt for supporting this work.

References

Shindy, 2017 – Shindy, H. A. (2017). *Dyes and Pigments*, 2017, 145, 505-513.

Shindy, 2016 – *Shindy, H.A.* (2016). *European Journal of Molecular Biotechnology*, 2016, 14 (4), 158-170.

Shindy, 2018 – Shindy, H.A. (2018). Dyes and Pigments, 2018, 149, 783-788.

Shindy, et. al., 2017 – *Shindy, H. A., Khalafalla, A. K., Goma, M. M. and Eed, A. H.* (2017). *European Journal of Molecular Biotechnology*, 5 (1), 30-42.

Shindy et al., 2017a – *Shindy, H. A., Khalafalla, A. K., Goma, M. M. and Eed, A. H.* (2017). European Reviews of Chemical Research, 2017, 4 (2), 52-65.

Solomon et al., 2014 – *Solomon, R.V., Jagadeesan, R., Vedha, S.A., Venuvanalingam, P.* (2014). Dyes and Pigment, 100, 261-268.

Lynch et al., 2013 – Lynch, D.E., Chowdhury, M.Z., Luu, N., Wane, E.S., Heptinstall, J., Cox, M. J. (2013). Dyes and Pigments, 96, 116-124.

Shindy, et. al., 2012 – *Shindy, H. A., El-Maghraby, M. A. and Eissa, F. M.* (2012). Dyes and Pigments, 92 (3), 929-935.

Arjona et al., 2016 – *Arjona, A., Stolte, M., Wilerthner, F.* (2016). Angewandte Chemie, 55 (7), 2470-2473.

Shindy et al., 2015 – *Shindy, H.A., Goma, M.M., Harb, N. A.* (2015). European Journal of Chemistry, 6 (2), 151-156.

Shindy, 2015 – *Shindy, H.A.* (2015). Revue Roumaine de Chimie, 60 (1), 5-13.

Shindy, Koraiem, 2008 – *Shindy, H.A., Koraiem, A.I.M.* (2008). Coloration Technology, 124 (5), 290-294.

Msaki, Tadashi, 1992 – *Msaki, O., Tadashi, I.* (1992). Chemical Abstract, 116, 245136r.

Mari, 1993 – *Mari, T.* (1993). Chemical Abstract, 119, 213939n.

Tadashi, 1992 – *Tadashi, O.* (1992). Chemical Abstract, 116, 48776y.

Nobuaki, 1995 – *Nobuaki, K.* (1995). Chemical Abstract, 123, 212968e.

Yoshio, Tadahire, 1999 – *Yoshio, I., Tadahire, T.* (1999). Chemical Abstract, 130, 117404d.

Toshiyoshi et. al., 2003 – *Toshiyoshi, U., Takuya, U., Yuji, M.* (2003). Chemical Abstract, 139, 14981w.

Tsutomu et al., 1994 – *Tsutomu, S., Tatsuya, T., Noboru, S.* (1994). Chemical Abstract, 121. 312163r.

Toshio, 1992 – *Toshio, I.* (1992). Chemical Abstract, 117, 9827s.

Hiroshi, 1999 – *Hiroshi, K.* (1999). Chemical Abstract, 130, 117428q.

Katsuji, Katsuhiko, 1991 – *Katsuji, A., Katsuhiko, K.* (1991). Chemical Abstract, 114, 64503w.

Rivera et al., 2007 – *Rivera, L., Puyol, M., Miltsov, S., Alonso, J.* (2007). Analytical and Bioanalytical Chemistry, 387, 2111-2119.

Clegg et. al., 1992 – *Clegg, R. M, Murchie, A. I., Zechel, A., Carlberg, C., Diekmann, S. and Lilley, D.M.* (1992). Biochemistry, 31: 4846-4856.

Norman et. al., 2000 – *Norman, D. G., Grainger, R. J., Uhrin, D., Lilley, D.M.* (2000). *Biochemistry* 39:6317-6324. [PubMed].

Mortensen, Chui, 2002 – *Mortensen, B., Chui, M.* (2002). *US. Pal. App. Publ.* 16.
Zhu, et. al., 1994 – *Zhu, H., Clark, S. M., Benson, S. C., Rye, II. S., Glazer, A. N. and Mathies, R. A.* (1994). *Anal. Chem.* 66: 1941-1984. [PubMed].
Schwartz, Ulfelder, 1992 – *Schwartz, H.E., Ulfelder, K.J.* (1992). *Anal. Chem.* 64: 1737-1740.
Bengtsson et al., 2003 – *Bengtsson, M., Karlsson, H. J., Westman, G., Kubista, M.* (2003). *Nucleic Acids Res.* 31: e45/1-e45/5. [PubMed]
Hirons et al. 1994 – *Hirons, G.T., Faweett, J.J., Crissman, H.A.* (1994). *Cytometry*. 15: 129-140. [PubMed].
Kurihara et al., 1977 – Kurihara, K., Toyoshima, Y. and Sukigara, M. (1977). *J Phys. Chem.* 81: 1833-1837.
Armitage, O'Brien, 1992 – *Armitage, B., O'Brien, D.F.* (1992). *J. Am. Chem. Soe*, 114: 7396-7403.
Reers et al., 1991 – Reers, M., Smith, T. W., and Chen, L. B. (1991). *Biochemistry*. 30: 4480-4486. [PubMed].
Panova, et. al., 2007 – *Panova, I. G., Sharova, N. P., Dmitrieva, S. B., Poltavtseva, R. A., Sukhikh, G. T., Tatikolov, A. S.* (2007). Analytical Biochemistry, 36 (2), 183-185.
Shindy, 2007 – *Shindy, H.A.* (2007). Coloration Technology, 123 (5), 298-305.
Wade, 1999 – *Wade Jr., L. G.* (1999). Organic. Chemistry., 4th Edn., Pearson Educ., (Prentice Hall, Upper Saddle River, New Jersy 07458, USA), 500-538.
Wade, 1999a – *Wade Jr., L. G.* (1999). Organic. Chemistry., 4th Edn., Pearson Educ., (Prentice Hall, Upper Saddle River, New Jersy 07458, USA), 544-560.
Shindy et al., 2002 – Shindy, H. A., El-Maghraby, M. A. and Eissa, F. M. (2002). Journal of the Chinese Chemical Society, 49, 1061-1068.
Shindy et al., 2006 – *Shindy, H. A., El-Maghraby, M. A., Eissa, F. M.* (2006). Dyes and Pigments, 70 (2) 2006, 110-116.
Shindy et al., 2015a – *Shindy, H. A., Khalafalla, A. K., Goma, M. M., Eed, A.H.* (2015). *European Reviews of Chemical Research,* 2015, 5 (3), 180-188.
Shindy et al., 2015b – *Shindy, H.A., Goma, M.M., Harb, N.A.* (2015). Revue Roumaine de Chimie, 60 (10), 965-974.
Gaspar et al., 2008 – *Gaspar, C. L., Panea, I. and Baldea, I.* (2008). Dyes and Pigments, 76, 455.
Green et al., 1992 – *Green, M.D., Patonay, G., Ndou, T. and Warner, I. M.* (1992). J. Inclusion Phenom. Macrocyclic Chem. 13, 181.

Appendix

Table 1. Characterization of the aza-cyanine (2a-c) and the bis aza-cyanine (3a-c) dyes

Comp. No.	Nature of products			Molecular formula (M. wt)	Analysis % calcd (found)			Visible electronic transitions in 95 % ethanol	
	m.p. °C	Yield %	Colour of crystals		C	H	N	λ_{max} (nm)	ε_{max} ($mol^{-1}cm^2$)
2a	168-170	93	Deep brown	$C_{36}H_{29}O_5N_5I_2$ (865)	49.94 (49.85)	3.35 (3.21)	8.09 (7.94)	390,425,475	13000,12100,11510
2b	173-175	82	Deep brown	$C_{40}H_{31}O_5N_5I_2$ (915)	52.46 (52.33)	3.39 (3.29)	7.65 (7.59)	395,430,480	14100,13020,12001
2c	188-190	95	Deep brown	$C_{40}H_{31}O_5N_5I_2$ (915)	52.46 (52.33)	3.39 (3.21)	7.65 (7.56)	400,435,485	16100,15010,17120
3a	178-180	80	Deep brown	$C_{42}H_{32}O_6N_6I_2$ (970)	51.95 (51.89)	3.29 (3.10)	8.65 (8.62)	405,440,490	18100,19200,11220
3b	218-220	85	Brown	$C_{50}H_{36}O_6N_6I_2$ (1070)	56.07 (56.00)	3.36 (3.34)	7.85 (7.81)	410,445,495	19121,21000,20000
3c	208-210	90	Deep brown	$C_{50}H_{36}O_6N_6I_2$ (1070)	56.07 (55.96)	3.36 (3.26)	7.85 (7.78)	415,450,500	20000,22000,27001

Table 2. IR and ^{1}H NMR spectral data of the prepared compounds

Comp. No.	IR (KBr, cm^{-1})	^{1}H NMR (DMSO, δ)
2a	649, 693 (monosubstituted benzene). 756, 850 (p.disubstituted benzene). 1024, 1123, 1188 (C–O–C cyclic). 1308, 1362 (C–N). 1623 (C=O quinone). 1597 (C=C). 1497, 1555 (C=N). 2922, 2852 (quaternary salts). 3425 (OH phenolic).	0.7-1.8 (m, 9H, 2 CH_3 of positions 3, 8 + 1 CH_3 of position 9). 3-4.3 (b, 4H, 2 CH_2 of positions 3, 8) 6.9 -8.4 (m, 16H, aromatic + 1 OH + 1 -CH=).
3a	649, 693 (monosubstituted benzene). 756, 851 (p.disubstituted benzene). 1023, 1122, 1187 (C–O–C cyclic). 1308, 1361 (C–N). 1624 (C=O quinone). 1597 (C=C). 1496, 1553 (C=N). 2927, 2853 (quaternary salts). 3425 (OH phenolic).	0.7-1.8 (t, 6H, 2 CH_3 of positions 3, 8). 2.9-4.3 (m, 4H, 2 CH_2 of positions 3, 8). 6.8-8.4 (m, 22H, aromatic + 2 OH + 2 -CH=).

Table 3. Solvent/electronic transitions correlation study of some selected aza-cyanine dye (2a) and bis aza-cyanine dye (3a) in pure solvents

Comp. No.	Water		Ethanol		DMF		Chloroform		Benzene		Dioxane	
	λ_{max} (nm)	ε_{max} ($mol^{-1}cm^2$)	λ_{max} (nm)	ε_{max} ($mol^{-1}cm^2$)	λ_{max} (nm)	ε_{max} ($mol^{-1}cm^2$)	λ_{max} (nm)	ε_{max} ($mol^{-1}cm^2$)	λ_{max} (nm)	ε_{max} ($mol^{-1}cm^2$)	λ_{max} (nm)	ε_{max} ($mol^{-1}cm^2$)
2a	370	12400	390	13000	420	15001	415	14000	405	13500	400	13400
	415	13500	425	12100	455	16100	450	15200	440	15000	430	14500
	--	--	475	11510	510	12510	505	12900	500	12800	490	12600
3a	370	20001	395	18100	420	20220	410	16010	405	14010	400	12100
	425	20201	430	19200	450	21570	440	15200	435	13010	425	11010
	--	--	480	11220	600	12100	590	11000	585	10300	485	10201

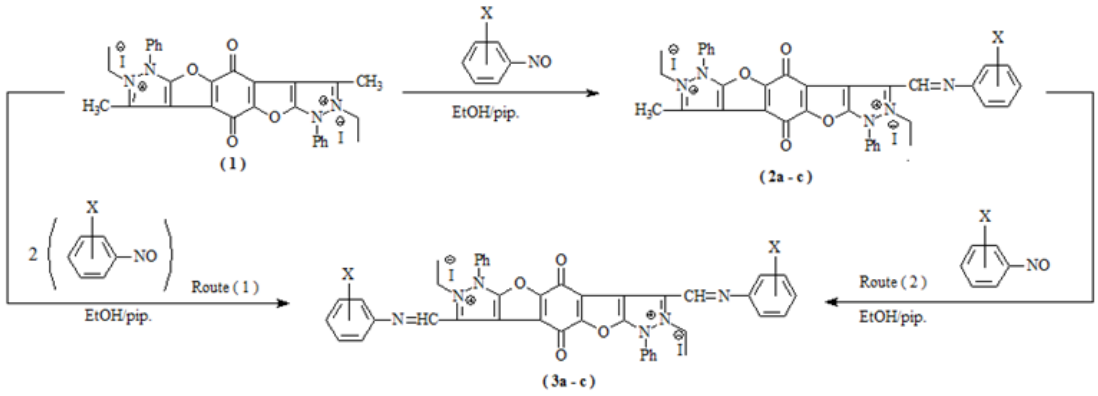

(2a - c); (3a - c): X = 4-OH (a); 2-OH, 5,6-benz (b); 2-OH, 3,4-benz (c).

Scheme (1)

Synthesis strategy of the prepared aza-cyanine dyes (2a-c) and bis aza-cyanine dyes (3a-c)

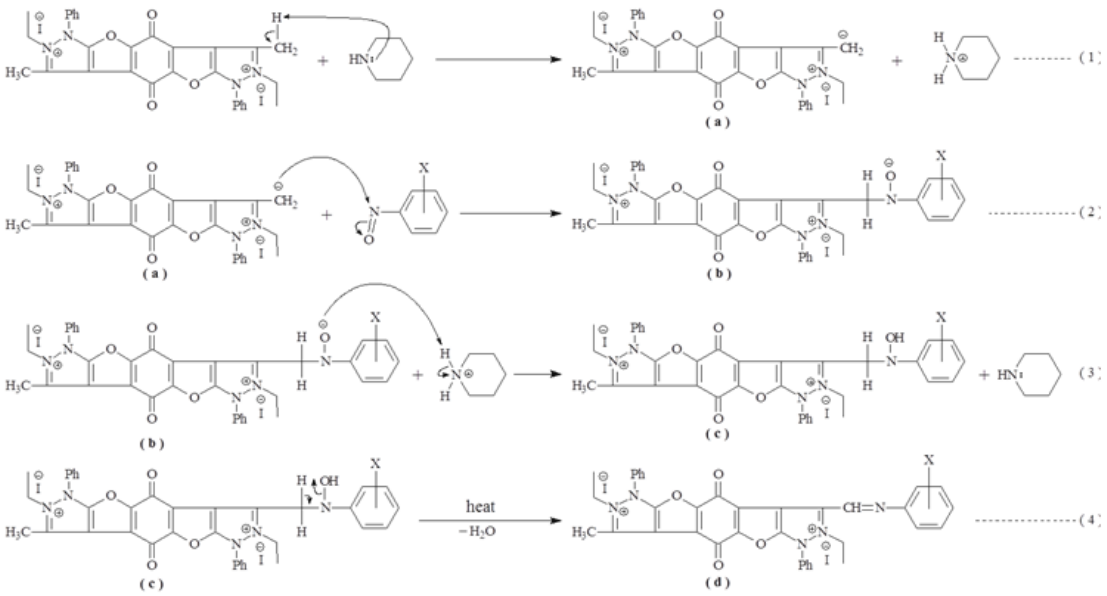

X = 4.OH; 2.OH, 5,6-benz; 2.OH,3,4-benz.

Scheme (2)

Synthesis mechanism of the aza-cyanine dyes (2a-c)

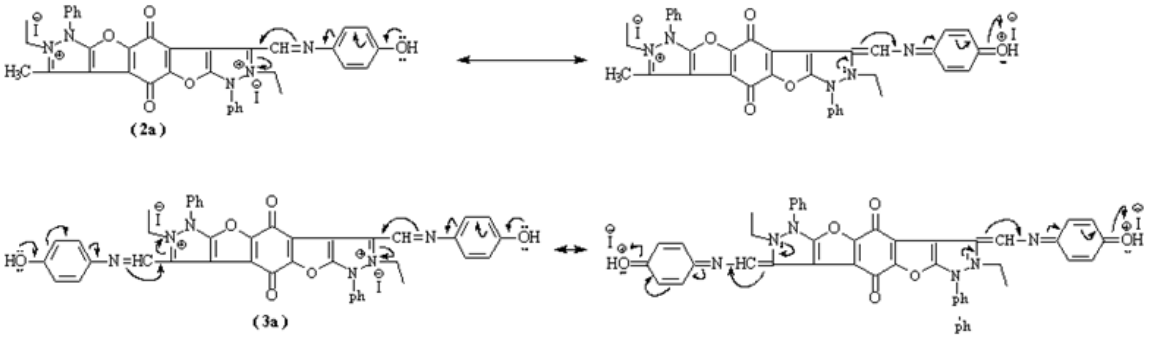

Scheme (3)

The colour intensity and/or the electronic charge transfer pathways illustration of the synthesized aza-cyanine dye (2a) and bis aza-cyanine dye (3a)

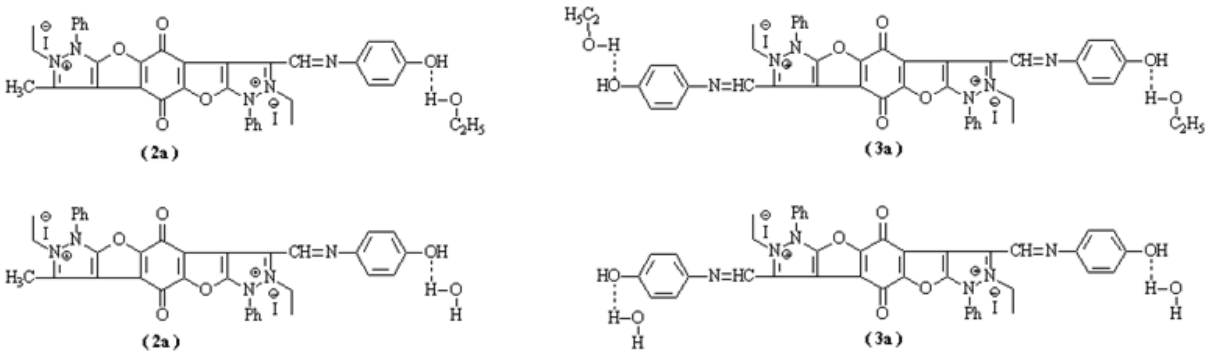

Scheme (4)

Hydrogen bond formation between the aza-cyanine dye (2a) and bis aza-cyanine dye (3a) with ethanol and water molecules (specific solvent effect)